Orphan nuclear receptor NR4A2 expressed in T cells from multiple sclerosis mediates production of inflammatory cytokines

Yoshimitsu Doi*, Shinji Oki*†, Tomoko Ozawa*, Hirohiko Hohjoh‡, Sachiko Miyake*, and Takashi Yamamura*†

Departments of *Immunology and ‡Molecular Genetics, National Institute of Neuroscience, National Center of Neurology and Psychiatry, 4-1-1 Ogawahigashi, Kodaira, Tokyo 187-8502, Japan

Communicated by Tadamitsu Kishimoto, Osaka University, Osaka, Japan, April 11, 2008 (received for review March 11, 2008)

Multiple sclerosis (MS) is an autoimmune disease of the central nervous system (CNS) mediated by Th17 and Th1 cells. DNA microarray analysis previously showed that NR4A2, an orphan nuclear receptor, is strongly up-regulated in the peripheral blood T cells of MS. Here, we report that NR4A2 plays a pivotal role for mediating cytokine production from pathogenic T cells. In experimental autoimmune encephalomyelitis (EAE), an animal model of MS, NR4A2, was selectively up-regulated in the T cells isolated from the CNS. Strikingly, a forced expression of NR4A2 augmented promoter activities of IL-17 and IFN-γ genes, leading to an excessive production of these cytokines. Conversely, treatment with siRNA for NR4A2, resulted in a significant reduction in the production of IL-17 and IFN-γ. Furthermore, treatment with NR4A2 siRNA reduced the ability of encephalitogenic T cells to transfer EAE in recipient mice. Thus, NR4A2 is an essential transcription factor for triggering the inflammatory cascade of MS/EAE and may serve as a therapeutic target.

IL-17 | interferon-γ | EAE | Th17 | siRNA

Multiple sclerosis (MS) is a chronic disease of the central nervous system (CNS), accompanying multiple foci of inflammatory lesions. MS is thought to have an autoimmune pathogenesis, involving autoimmune T cells reactive to myelin antigens (1). Development of the CNS inflammation is triggered by proinflammatory cytokines produced by the autoimmune T cells, which penetrate into the CNS parenchyma after being activated in the periphery (2, 3). Although the precise mechanism for the peripheral T cell activation remains obscure, studies indicated possible roles for cross-reactive peptides, cytokines, or superantigen (4).

Experimental autoimmune encephalomyelitis (EAE) is a prototype autoimmune disease model (5) that can be induced in laboratory animals by active immunization with myelin antigens (mAg) or by passive transfer of mAg-specific T cells. Because Th1 cell clones reactive to mAg are capable of inducing clinical and pathological manifestations of EAE in naive mice, it has long been believed that Th1 cells producing IFN-γ play a central role in the pathogenesis of EAE and MS. This postulate is also supported by the past experience that clinical application of IFN-γ treatment for MS turned out to worsen the disease (6). Furthermore, treatment with a peptide analogue of myelin basic protein (MBP) resulted in disease exacerbation along with an expansion of MBP-reactive Th1 cells (7). These results have been repeatedly mentioned to support the Th1-mediated pathogenesis of MS. However, this dogma has recently been challenged. Namely, despite an obvious reduction of Th1 cells, mice deficient for IFN-γ or IFN-γ receptor (8) or for IL-12 signaling were susceptible to EAE (9, 10). Subsequent studies have clarified that IL-23 rather than IL-12 is essential for EAE induction. Lately, the IL-23-dependent pathogenic T cells were identified as Th17 cells, a novel helper T cells producing IL-17 (11, 12). Currently, it is widely appreciated that Th17 cells are crucial in the development of autoimmune diseases either independently or collaboratively with Th1 cells (13).

DNA microarray analysis revealed an up-regulation of IL-17 in the brain lesions of MS (14). More recently, a pathological study has demonstrated that IL-17 secreting T cells are present in active lesions of MS (15). Gene expression profiling provided a number of potential candidate molecules that might be appropriate as a therapeutic target (14, 16). We recently characterized gene signature of peripheral blood T cells from Japanese MS patients and found that a nuclear orphan receptor NR4A2 is most significantly overexpressed in MS (17). NR4A2 mutations are reported to cause familial Parkinson's disease, reflecting its essential role in the development and survival of substantia nigra neurons (18). In contrast, much less attention has been paid onto its role in T cells. NR4A family members (NR4A1 and -3) were shown to mediate apoptotic processes of mature (19, 20) and immature T cells (21, 22). However, these studies do not give insights into an overexpressed NR4A2 in MS. Here, we report that NR4A2 is a transcription factor regulating the expression of key cytokines in the pathogenesis of MS, including IL-17. Furthermore, we revealed that silencing NR4A2 expression by specific siRNA effectively prevents the production of the cytokines, thereby inhibiting their pathogenic potentials to mediate EAE.

Results

Up-Regulation of NR4A2 in Peripheral Blood T Cells of MS. We analyzed gene expression profiles of peripheral blood T cells from MS and control subjects (17, 23). Comparison of the patients and healthy donors has revealed that 286 of 1,263 genes are differentially expressed between MS and controls. Among genes up-regulated in MS, NR4A2 was most significantly overexpressed in MS in statistical P values and an increase ratio (3.6-fold). To consolidate the overexpression of NR4A2 in MS, we performed quantitative RT-PCR for NR4A2 expression, using the same samples previously analyzed. Expression of NR4A2 in T cells from MS increased ≈5-fold on average compared with healthy donors (Fig. 1; $P < 0.01$).

T Cell Expression of NR4A2 in EAE. NR4A2 is a transcription factor of steroid/thyroid receptor family implicated in various cellular responses such as steroidogenesis, neuronal development, atherogenesis, and cell cycle regulation (24). However, its role in

Author contributions: Y.D., S.O., H.H., S.M., and T.Y. designed research; Y.D., S.O., and T.O. performed research; Y.D., S.O., S.M., and T.Y. analyzed data; and S.O. and T.Y. wrote the paper.

The authors declare no conflict of interest.

Freely available online through the PNAS open access option.

†To whom correspondence may be addressed. E-mail: soki@ncnp.go.jp or yamamura@ncnp.go.jp.

This article contains supporting information online at www.pnas.org/cgi/content/full/0803454105/DCSupplemental.

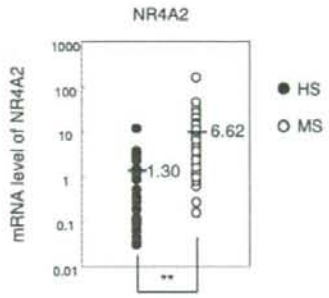

Fig. 1. Quantitative analysis of NR4A2 transcription between MS and controls. CD3+ T cells were isolated from PBMC of 57 MS patients and of 19 healthy donors, and total RNA was extracted. cDNA was synthesized and the expression levels of NR4A2 transcript were analyzed by quantitative RT-PCR. Each sample was normalized to GAPDH to adjust for variations. Open circles, MS patients; filled circles, healthy controls. Bars indicate mean values of each group. The statistical difference was determined by two-sided Student *t* test (**, $P < 0.01$).

T cell-mediated autoimmune diseases is unknown. Therefore, we explored the functional involvement of NR4A2 in EAE induced in C57BL/6 (B6) mice by immunization with MOG_{35-55}. $CD3^+$ T cells were isolated from SPL, dLN, and PBMC after EAE induction and the expression levels of NR4A2 gene were measured by quantitative RT-PCR (Fig. 2*a Right*). NR4A2 expression was detectable in PBMC-T cells on days 14, 21, and 28, showing a maximum value on day 21, which was well correlated with the clinical severity of EAE (Fig. 2*a Left*). NR4A2 expression in SPL-T cells and dLN-T cells was also correlated with the severity of EAE, but only marginally.

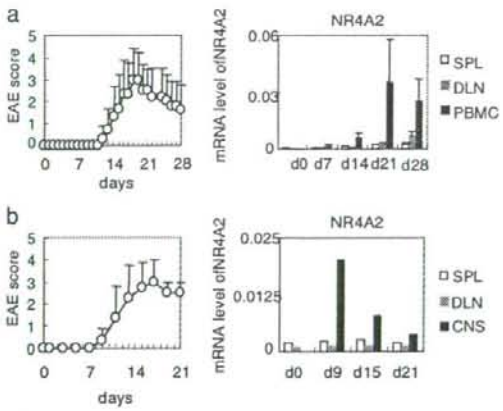

Fig. 2. Kinetic analysis of NR4A2 expression in the disease course of EAE. (*a*) (*Left*) EAE was induced in B6 mice by immunization with MOG_{35-55} in CFA. Mice were killed on days 7, 14, 21 and 28 after immunization, and T cells were isolated from dLN, SPL, or PBMC, using anti-CD3 magnetic beads. (*Right*) Total RNAs were isolated from the T cell populations, and the expression levels of NR4A2 were determined by quantitative RT-PCR. One representative data from three independent experiments is shown, and data are expressed as mean ± SEM ($n = 5$ for each). (*b*) EAE induced in B6 mice with MOG_{35-55}. Clinical scores were expressed as mean ± SEM ($n = 4$). Here, we determined NR4A2 expression in $CD3^+$ T cells isolated by using EPICS ALTRA cell sorter. The lymphoid cells (SPL, dLN, and CNS) were pooled from four mice on days 0, 9, 15, and 21 and used for cell sorting and RT-PCR analysis. The purity of the CNS-derived $CD3^+$ T cells was >93%.

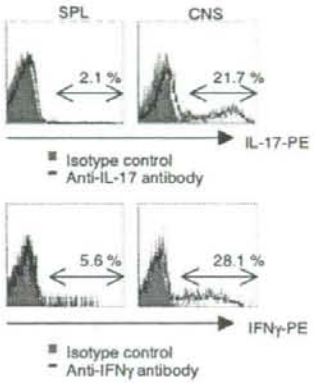

Fig. 3. Accumulation of IL-17 or IFN-γ-producing inflammatory T cells in the CNS. Mononuclear cells were isolated from spleen or CNS on day 17 after immunization and stimulated with PMA (20 ng/ml) and ionomycin (1 μg/ml) in the presence of 2 mM monensin for 4 h. Production of IL-17 and IFN-γ was analyzed for the gated $CD4^+$ T cell population by intracellular cytokine staining. Black line represents samples stained with either anti-IL-17 or anti-IFN-γ Ab, and the filled histogram represents samples stained with isotype control. Given values show the percentage of cytokine producing-T cells present in each panel.

In the course of EAE, mAg-primed T cells would accumulate into the CNS and produce inflammatory cytokines, leading to the formation of inflammatory lesions (25). We next examined a kinetic change of NR4A2 in the T cells infiltrating into the CNS. As assessed by quantitative RT-PCR, remarkable expression of NR4A2 was observed in the CNS-T cells on day 9, when an early EAE sign became evident (Fig. 2*b*). The expression level decreased gradually thereafter, but was still significant until day 21. These results suggest that the CNS-T cells also express NR4A2, but the expression kinetics significantly differed from that of PBMC-T cells.

Accumulation of IL-17- and IFN-γ-Producing T Cells in the CNS of EAE. Th1 cells specific for mAg have long been thought to induce EAE through their production of IFN-γ. However, recent studies indicate that Th17 rather than Th1 cells may play a central role (13). To make this point clear in our experimental setting, we examined the ability of the CNS-T cells to produce IFN-γ and IL-17. Mononuclear cells were recovered from the CNS and SPL on day 17, and stimulated with PMA and ionomycin (P/I). After immunostaining, expression of IL-17 or IFN-γ in the $CD4^+$ T cells was analyzed by flow cytometry. Major proportions of the CNS-T cells were found to produce IL-17 (21.7% of the cells) or IFN-γ (28.1%) after stimulation (Fig. 3). In contrast, spleen cells contained a lower number of cells producing these cytokines.

Transcriptional Up-Regulation of IL-17 and IFN-γ After Introduction of NR4A2. The concomitant expression of inflammatory cytokines and NR4A2 has guided us to investigate whether NR4A2 directly affects cytokine gene expression as a transcription factor, using luciferase reporter plasmids containing the promoter fragment of IL-17, IFN-γ, or IL-2. NR4A2 gene transduction would result in a twofold augmentation of IL-17 promoter activity and, for IFN-γ, an even higher (5-fold) induction (Fig. 4*a*). A significant induction of IL-2 promoter activity was also noted. Intriguingly, an introduction of NR4A2 plasmid

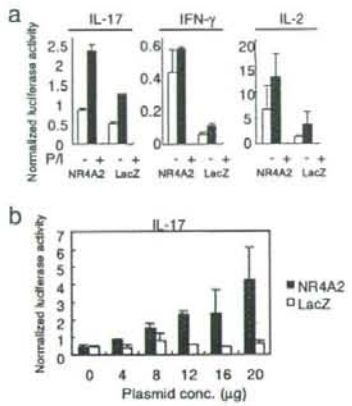

Fig. 4. Promoter activities of cytokine genes in the presence of NR4A2. (*a*) The effect of NR4A2 expression on IL-17, IFN-γ, and IL-2 promoter activity. A reporter plasmid containing promoter of cytokine gene (10 μg) and *Renilla* luciferase plasmid (100 ng) were introduced into EL4 cells by electroporation, together with pcDNA4-NR4A2 or pcDNA4-LacZ (10 μg). Cells were stimulated for 18 h with P/I. Luciferase activity was determined for each cell lysate after normalization to the *Renilla* luciferase activity. One representative data from three independent experiments is shown. Data are expressed as mean ± SD. (*b*) The effect of NR4A2 expression on basal promoter activity of IL-17 gene. EL4 cells transfected with pcDNA4-NR4A2 or pcDNA4-LacZ together with IL-17 reporter plasmid and *Renilla* luciferase plasmid as desribed in *a* were cultured for 18 h without stimulation. One representative data from three independent experiments is shown. Data are expressed as mean ± SD.

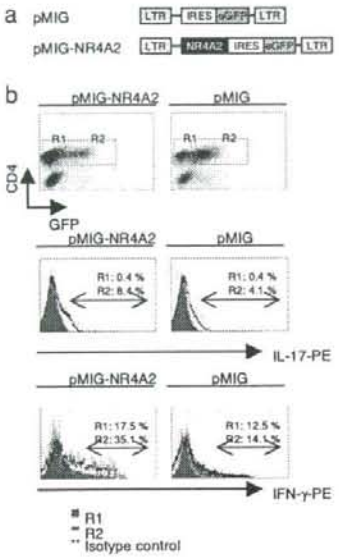

Fig. 5. The effect of retrovirally transduced NR4A2 on cytokine production by primary murine CD4⁺ T cells. (*a*) DNA fragments encoding wild-type NR4A2 were cloned into the pMIG(W) bicistronic retroviral vector. LTR, long terminal repeat; IRES, internal ribosome entry site; eGFP, enhanced green fluorescence protein b. (*b*) Splenic CD4⁺ T cells were infected with retrovirus encoding NR4A2 or control retrovirus, and CD4⁺ GFP⁻ T cells and CD4⁺ GFP⁺ T cells were gated as R1 and R2, respectively. Forced expression of NR4A2 increased the number of CD4⁺ T cells producing IL-17 or IFN-γ. The histogram shows intracellular cytokine staining on the gated cells (R1 or R2). Black line represents cells in R2 gate (GFP+) stained with either anti-IL-17 or anti-IFN-γ Ab, and the filled histogram represents cells in R1 gate (GFP−) stained with isotype control. Given values show the percentage of cytokine producing-T cells present.

without P/I stimulation also augmented basal promoter activity of IL-17 genes in a dose dependent manner (Fig. 4*b*). Similarly, basal promoter activity of IFN-γ was promoted (data not shown).

Retroviral Transduction of NR4A2 Gene Enhances Expression of Inflammatory Cytokine in Primary T Cells. The results obtained in EL4 lymphoma cells need to be verified in more physiological settings. Next, we examined whether forced expression of NR4A2 may affect the expression of cytokines in primary rodent T cells. Bicistronic retroviral vector containing NR4A2 gene fragment (pMIG-NR4A2) or empty vector (pMIG) were used for production of retroviruses (Fig. 5*a*). We infected the B6 T cells with either of the retroviruses as described in ref. 26 and compared the cytokine production between GFP-positive (infected) and GFP-negative (uninfected) CD4⁺ T cells by intracellular cytokine staining (Fig. 5*b Top*). CD4⁺ T cells infected with pMIG-NR4A2-introduced retrovirus showed a twofold enhancement of IL-17 expression (8.4%) compared with those infected with control retrovirus (4.1%) after stimulation with P/I. In contrast, IL-17 production by uninfected T cells in either panel was almost equivalent (Fig. 5*b Middle*). Furthermore, one-third of the CD4⁺ T cells infected with pMIG-NR4A2-introduced retrovirus showed a massive IFN-γ expression (35.1%) compared with control retrovirus (14.1%) (Fig. 5*b Bottom*).

Silencing of NR4A2 Gene Expression Results in a Reduced Production of IL-17 and IFN-γ. Reporter gene analysis and retroviral transduction experiments demonstrated that T cell production of IL-17 and IFN-γ is controlled by NR4A2 (Figs. 4 and 5). We further explored whether silencing of NR4A2 gene may affect the production of inflammatory cytokines by CD4⁺ T cells. An NR4A2-specific siRNA was selected from three siRNAs based on the inhibitory efficacy. The targeting sequence of the NR4A2 siRNA is completely conserved between mice and human. Therefore, we could apply it to human T cells and study whether NR4A2 could be a therapeutic target in human MS. In a preparatory experiment, using FITC-labeled siRNA, the transfection efficiency was found to be 95%. We purified CD4⁺ T cells from human PBMC and transfected them with the NR4A2 siRNA or control RNA, using nucleofector II. The cells were stimulated with immobilized anti-CD3 Ab. As shown in Fig. 6*a*, silencing NR4A2 gene expression resulted in a 50% reduction of IL-17 and IFN-γ production. However, production of TNF-α, IL-4, or IL-5 was not changed significantly after siRNA treatment (Fig. 6*b*). Intriguingly, the siRNA treatment also induced a modest reduction of IL-10 production. The molecular mechanism of this inhibition is not clarified yet. Because silencing of NR4A2 expression rather selectively inhibited the expression of inflammatory cytokines, it is arguable that NR4A2 may be a good target for therapeutic intervention of MS. In this line, we next examined whether the NR4A2 siRNA is effective for inhibiting a production of inflammatory cytokines in MS. For this aim, CD4⁺ T cells were isolated from pairs of an MS patient and an age- and sex-matched healthy donor and were stimulated with anti-CD3 Ab after being transfected with the NR4A2 siRNA or control RNA. We found that the siRNA treatment significantly reduced the production of IL-17 and IFN-γ by T cells from MS or healthy donors [supporting information (SI) Fig. S1]. Again we observed some reduction of IL-10 after siRNA treatment. However, the siRNA showed little effect on

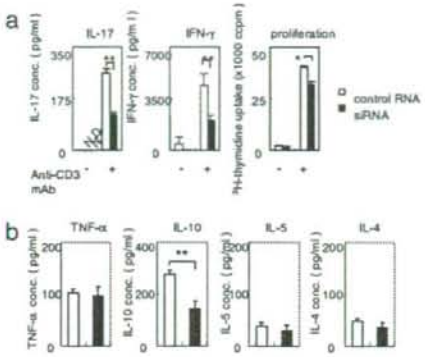

Fig. 6. The effect of NR4A2 gene silencing on T cell cytokine production. (*a*) Specific inhibition of T cell production of IL-17 and IFN-γ by siRNA treatment. Human CD4⁺ T cells derived from PBMC were transfected with siRNA or control RNA and stimulated by immobilized anti-CD3 Ab for 48 h. Cytokine levels in the culture supernatant were determined by ELISA or a CBA human Th1/2 cytokine kit. Proliferation rate was measured by ^{3}H-TdR uptake. (*b*) Effect of siRNA treatment for T cell production of TNF-α, IL-10, IL-5, and IL-4 after stimulation with immobilized anti-CD3 Ab. The data are expressed as mean ± SD (•, $P < 0.05$; ••, $P < 0.01$; Mann–Whitney *U* test).

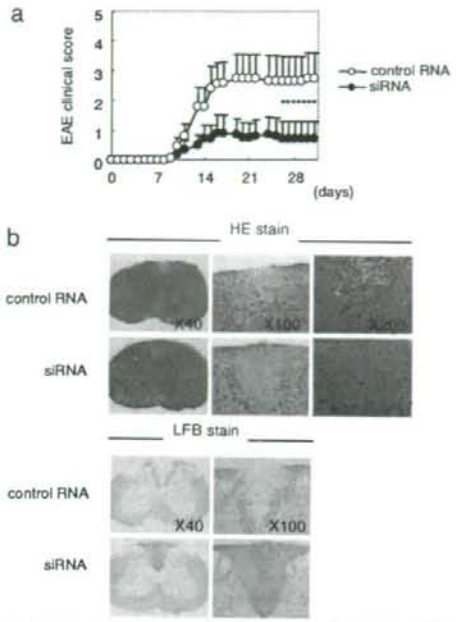

Fig. 7. The effect of T cell silencing of NR4A2 expression on passive EAE. (*a*) Inguinal and popliteal LNs cells were collected from female SJL/J mice 10 days after immunization with $PLP_{139-151}$, and were transfected with siRNA for NR4A2 or control RNA, using HVJ-E vector kit. The cells were cultured in complete media for 8 h. Then the media were replaced with fresh complete media containing 35 μg/ml $PLP_{139-151}$, and the cells were stimulated for another 3 days. After expansion, cells were harvested and transferred i.p. (5×10^6 cells per mouse) into 3Gy-irradiated naïve SJL/J mice ($n = 10$) followed by i.p. injection of PT. Mean ± SEM clinical scores were indicated. (•, $P < 0.05$ by Mann–Whitney *U* test.) (*b*) Histological analysis of spinal cords removed on day 31 after adoptive transfer of $PLP_{139-151}$-reactive T cells. Sections obtained from cervical cord regions were stained with HE or LFB. Infiltration of mononuclear cells and demyelination of the cervical cord regions were analyzed for mice injected with $PLP_{139-151}$-reactive T cells pretreated with control RNA or siRNA for NR4A2.

production of TNF-α, IL-5, and IL-4 from T cells used for assays (Table S1).

Amelioration of EAE by Silencing of NR4A2. Finally, we investigated the therapeutic implication of the siRNA experiments in a model of passively induced EAE, induced by adoptive transfer of mAg-activated LN cells. We prepared lymphoid cells from dLN of SJL/J mice 10 days after immunization with $PLP_{139-151}$. The dLN cells were transfected with the NR4A2 siRNA or control RNA and stimulated with $PLP_{139-151}$ *in vitro*. Three days later, the cultured cells enriched in lymphoblasts were transferred to irradiated naïve SJL/J mice. In addition to evaluating clinical manifestations, histology was assessed by hematoxylin-eosin (HE) and luxol fast blue (LFB) staining of paraffin-embedded spinal cord sections. Notably, severity of clinical (Fig. 7*a*) and histological EAE on day 31 (Fig. 7*b*) was significantly prevented in siRNA-treated group compared with control RNA-treated group (Fig. 7*b*). These results suggest that modulation of NR4A2 expression by specific siRNAs or other chemical compounds might be a promising treatment for active MS that are harboring potent encephalitogenic T cells.

Discussion

Although mAg-specific T cell clones isolated from the peripheral blood has been widely used to gain insights into the pathogenesis of MS (27), analysis of polyclonal T cells has been undervalued for a long time. However, it was recently demonstrated that peripheral T cells from MS and healthy subjects significantly differ in surface phenotype or gene expression profiling (17, 23, 28). Using cDNA microarray, we have identified NR4A2 as a gene most significantly up-regulated in the peripheral T cells of MS (17). We conducted the present study to clarify the implication of this interesting observation. Inspired by the recent discovery that retinoid-related orphan receptor γt (RORγt) is essential for Th17 cell differentiation (29) and that retinoic acids play a regulatory role in Th17 cell differentiation (30), we have focused our efforts to explore the possible role of NR4A2 in cytokine regulation. Reporter gene analysis and retroviral transduction of NR4A2 clearly demonstrated that T cell production of inflammatory cytokines, including IL-17 and IFN-γ, is regulated by NR4A2, whereas silencing of NR4A2 by a specific siRNA prevents expression of these cytokines. Furthermore, treatment with the siRNA reduced the ability of pathogenic T cells to adoptively transfer EAE. These results have identified a previously uncharacterized role for NR4A2 in the regulation of T cell production of inflammatory cytokines.

NR4A2 is a member of the orphan nuclear NR4A subfamily that consists of NR4A1 (also referred to as Nur77), NR4A2 (Nurr1), and NR4A3 (NOR-1) (24). The NR4A members share a highly conserved zing finger DNA binding domain and a less conserved putative ligand-binding domain. All these members bind to the DNA sequence NBRE (AAAGGTCA) or NurRE to activate target gene expression. NR4A1 and NR4A2 can also heterodimerize with retinoic X receptor (RXR) and activate gene expression through DR5 (24). They exert pleiotropic functions and are classified as immediate early genes induced by physiological and physical stimuli. Studies of gene-targeted mice have shown that NR4A1 and NR4A3 play a critical role in T cell apoptosis during the thymocyte development (20–22, 31). In contrast, developing thymocytes in NR4A2 deficient mice ap-

pear to be normal (21, 32), which distinguishes NR4A2 from other NR4A members.

Involvement of orphan nuclear receptor in T cell differentiation has recently attracted broad attention, because RORγt, a splice variant of RORγ, was found to play an essential role in the development of Th17 cells (29). RORγ/RORγt were reported to play an essential function in survival of $CD4^+CD8^+$ thymocytes (33, 34) and in the generation of fetal lymphoid tissue inducer (LTi) cells (35). It is particularly intriguing that the consensus binding sequence for RORγ [$(A/T)_5$AGGTCA] overlaps with that for NR4A (NBRE; AAAGGTCA), which has encouraged us to explore the functional role of NR4A2 in the production of IL-17 and IFN-γ. Although the molecular mechanism of cytokine production through the induced expression of NR4A2 is not clear yet, NR4A2 and RORγt may have an overlapping role in regulating the development and effector functions of Th17 cells.

NR4A2 expression in the CNS-infiltrating T cells showed a peak value at a very early phase of EAE (day 9–12) (Fig. 2*b*). We speculate that this probably coincides with the entry of encephalitogenic cells into the CNS (2, 3). Consistently, a similar kinetic change was found in expression of T-bet and RORγt in the CNS-T cells (data not shown). In contrast, up-regulation of NR4A2 in peripheral blood T cells was significantly delayed. This is likely to result from a late activation of peripheral T cells after peripheral recruitment of antigen presenting cells engulfing myelin and/or peripheral dispersion of myelin protein or its fragments.

By applying a specific siRNA, we showed that blocking NR4A2 expression is effective for inhibiting production of IL-17 and IFN-γ from T cells from healthy donors and MS patients. Therapeutic implication was further demonstrated by using an adoptive transfer EAE model. Because Th17 cells were identified as a major player in autoimmunity (12, 15), it is sometimes argued that Th17 cells would be a sole potent inducer of autoimmune inflammation. However, T-bet-deficient mice and Stat4-deficient mice that obviously lack Th1 cells would resist against induction of EAE, although they maintain a large number of Th17 cells (36, 37). This suggests that both Th1 and Th17 cells are required for induction of full-blown EAE (38). In this context, the ability of the NR4A2 siRNA to inhibit production of both IL-17 and IFN-γ suggests the advantage of NR4A2 targeting therapy in controlling autoimmune inflammation.

Materials and Methods

EAE Induction. Active EAE was induced with myelin oligodendrocyte glycoprotein (MOG) amino acids 35–55 (MOG_{35-55}; MEVGWYRSPFSRVVHLYRNGK) as described in ref. 39. Female B6 mice were immunized s.c. with 100 μg of MOG_{35-55} mixed with 1 mg of heat-killed *Mycobacterium tuberculosis* H37RA emulsified in Freund's adjuvant (CFA). Pertussis toxin (PT) (200 ng) was injected i.p. on days 0 and 2 after immunization. Clinical signs were scored daily as follows: 0, no clinical signs; 1, loss of tail tonicity; 2, flaccid tail; 3, partial hind limb paralysis; 4, total hind limb paralysis; and 5, fore and hind limb paralysis.

Quantitative RT-PCR. DNase-treated total RNAs were processed for cDNA synthesis, using random hexamer primers and SuperScript II reverse transcriptase (Invitrogen). cDNAs were amplified by PCR on Light Cycler ST300 (Roche Diagnostics) by using a Light Cycler-FastStart DNA Master SYBR Green I kit (Roche). Values for each gene were normalized to those of a housekeeping gene GAPDH to adjust for variations between different samples. Forward primer for amplifying human NR4A2 gene was 5′-CGACATTTCTGCCTTCTCC-3′ and reverse primer 5′-GGTAAAGTGTCCAGGAAAAG-3′. Mouse NR4A2 forward primer was designed as 5′-GCATACAGGTCCAACCCAGT-3′ and reverse primer 5′-AATGCAGGAGAAGGCAGAAA-3′. To evaluate silencing efficacy of *NR4A2*-specific siRNAs, expression of NR4A2 gene was quantified by RT-PCR, using the primers to flank the siRNA target sequence (forward, 5′-TGCCACCACTTCTCTCCCCA-3′; reverse, 5′-GCGGCATCATCTCCTCAGAC-3′).

Luciferase Assays. Ten million of EL4 thymoma cells suspended in 500 μl of cold PBS and transfected with 4–20 μg of pcDNA4-NR4A2 or pcDNA4-LacZ in the presence of 10 μg of reporter plasmid, 100 ng of Renilla luciferase plasmid, and 5 μg of DEAE-DEXTRAN (Sigma) by electroporation (250 V, 975 μF, time constant = 30–34 ms) with a GenePulser electroporator II (Bio-Rad). Six hours later, cells were stimulated with 20 ng/ml PMA and 1 μg/ml ionomycin for 24 h, followed by analysis for luciferase activity. The data were normalized for internal controls of Renilla luciferase activity.

Retroviral Infection. Mouse $CD4^+$ T cells purified by AutoMACS using mouse CD4 T isolation kit (Miltenyi Biotec) were stimulated with immobilized anti-CD3 Ab and soluble anti-CD28 Ab in complete medium supplemented with IL-2 (100 units/ml) for 24–48 h before infection. The primed $CD4^+$ T cells were infected twice with retroviruses produced by 293T cells cotransfected with pMIG retroviral vector and pCL-Eco packaging vector. The T cells were cultured in the presence of 30 units/ml of IL-2 for 3 days and were then subjected to intracellular cytokine staining.

Silencing Effects of NR4A2 siRNA on Passive EAE. To evaluate an effect of NR4A2 siRNA, an adoptive transfer EAE model in SJL/J mice was applied, because consistent disease could be induced relatively easily. Female SJL/J mice (8–12 weeks old) (Charles River Laboratories) were immunized s.c. with 100 μg of proteolipid protein (PLP) amino acids 139–151 ($PLP_{139-151}$; HSLGKWLGHPDKF) and 1 mg of heat-killed *M. tuberculosis* H37RA in CFA. Inguinal and popliteal LNs harvested 10 days after immunization were transfected with siRNAs, using hemaggultinating Virus of Japan envelope (HVJ-E) vector kit (GENOMEONE; Ishihara Sangyo). Eight hours later, the cells were stimulated with $PLP_{139-151}$ peptide (35 μg/ml). After 3 days, collected cells were injected i.p. (5×10^6 cells per body) into irradiated mice (3 Gy/body) with intrapelitoneal injection of PT. For conventional histological analysis of EAE, paraffin-embedded spinal cords were stained with either HE or LFB.

Statistics. For statistical analysis, a nonparametric Mann–Whitney *U* test or Student *t* test was used. $P < 0.05$ was considered statistically significant.

Supporting Information. For further details, see *SI Materials and Methods*.

ACKNOWLEDGMENTS. We thank Mayumi Fujita for EAE induction, Miho Mizuno, Chiharu Tomi, and Yuki Kikai for excellent technical assistance. This work was supported by grants from the Ministry of Health, Labour and Welfare of Japan.

1. Sospedra M, Martin R (2005) Immunology of multiple sclerosis. *Annu Rev Immunol* 23:683–747.
2. Hickey WF, Hsu BL, Kimura H (1991) T-lymphocyte entry into the central nervous system. *J Neurosci Res* 28:254–260.
3. Kawakami N, *et al.* (2005) Live imaging of effector cell trafficking and autoantigen recognition within the unfolding autoimmune encephalomyelitis lesion. *J Exp Med* 201:1805–1814.
4. Hur EM, *et al.* (2007) Osteopontin-induced relapse and progression of autoimmune brain disease through enhanced survival of activated T cells. *Nat Immunol* 8:74–83.
5. Gold R, Linington C, Lassmann H (2006) Understanding pathogenesis and therapy of multiple sclerosis via animal models: 70 years of merits and culprits in experimental autoimmune encephalomyelitis research. *Brain* 129:1953–1971.
6. Panitch HS, Hirsch RL, Schindler J, Johnson KP (1987) Treatment of multiple sclerosis with gamma interferon: Exacerbations associated with activation of the immune system. *Neurology* 37:1097–1102.
7. Bielekova B, *et al.* (2000) Encephalitogenic potential of the myelin basic protein peptide (amino acids 83–99) in multiple sclerosis: Results of a phase II clinical trial with an altered peptide ligand. *Nat Med* 6:1167–1175.
8. Willenborg DO, Fordham S, Bernard CC, Cowden WB, Ramshaw IA (1996) IFN-gamma plays a critical down-regulatory role in the induction and effector phase of myelin oligodendrocyte glycoprotein-induced autoimmune encephalomyelitis. *J Immunol* 157:3223–3227.
9. Becher B, Durell BG, Noelle RJ (2002) Experimental autoimmune encephalitis and inflammation in the absence of interleukin-12. *J Clin Invest* 110:493–497.
10. Zhang GX, *et al.* (2003) Induction of experimental autoimmune encephalomyelitis in IL-12 receptor-beta 2-deficient mice: IL-12 responsiveness is not required in the pathogenesis of inflammatory demyelination in the central nervous system. *J Immunol* 170:2153–2160.
11. Cua DJ, *et al.* (2003) Interleukin-23 rather than interleukin-12 is the critical cytokine for autoimmune inflammation of the brain. *Nature* 421:744–748.
12. Langrish CL, *et al.* (2005) IL-23 drives a pathogenic T cell population that induces autoimmune inflammation. *J Exp Med* 201:233–240.
13. Bettelli E, Korn T, Kuchroo VK (2007) Th17: The third member of the effector T cell trilogy. *Curr Opin Immunol* 19:652–657.
14. Lock C, *et al.* (2002) Gene-microarray analysis of multiple sclerosis lesions yields new targets validated in autoimmune encephalomyelitis. *Nat Med* 8:500–508.

15. Tzartos JS, *et al.* (2008) Interleukin-17 production in central nervous system-infiltrating T cells and glial cells is associated with active disease in multiple sclerosis. *Am J Pathol* 172:146–155.
16. Lock CB, Heller RA (2003) Gene microarray analysis of multiple sclerosis lesions. *Trends Mol Med* 9:535–541.
17. Satoh J, *et al.* (2005) Microarray analysis identifies an aberrant expression of apoptosis and DNA damage-regulatory genes in multiple sclerosis. *Neurobiol Dis* 18:537–550.
18. Le WD, *et al.* (2003) Mutations in NR4A2 associated with familial Parkinson disease. *Nat Genet* 33:85–89.
19. Liu ZG, Smith SW, McLaughlin KA, Schwartz LM, Osborne BA (1994) Apoptotic signals delivered through the T-cell receptor of a T-cell hybrid require the immediate-early gene nur77. *Nature* 367:281–284.
20. Woronicz JD, Calnan B, Ngo V, Winoto A (1994) Requirement for the orphan steroid receptor Nur77 in apoptosis of T-cell hybridomas. *Nature* 367:277–281.
21. Cheng LE, Chan FK, Cado D, Winoto A (1997) Functional redundancy of the Nur77 and Nor-1 orphan steroid receptors in T-cell apoptosis. *EMBO J* 16:1865–1875.
22. Calnan BJ, Szychowski S, Chan FK, Cado D, Winoto A (1995) A role for the orphan steroid receptor Nur77 in apoptosis accompanying antigen-induced negative selection. *Immunity* 3:273–282.
23. Satoh J, *et al.* (2006) T cell gene expression profiling identifies distinct subgroups of Japanese multiple sclerosis patients. *J Neuroimmunol* 174:108–118.
24. Maxwell MA, Muscat GE (2006) The NR4A subgroup: Immediate early response genes with pleiotropic physiological roles. *Nucl Recept Signal* 4:e002.
25. Hofstetter HH, Toyka KV, Tary-Lehmann M, Lehmann PV (2007) Kinetics and organ distribution of IL-17-producing CD4 cells in proteolipid protein 139–151 peptide-induced experimental autoimmune encephalomyelitis of SJL mice. *J Immunol* 178:1372–1378.
26. Oki S, Chiba A, Yamamura T, Miyake S (2004) The clinical implication and molecular mechanism of preferential IL-4 production by modified glycolipid-stimulated NKT cells. *J Clin Invest* 113:1631–1640.
27. Meinl E, *et al.* (1993) Myelin basic protein-specific T lymphocyte repertoire in multiple sclerosis. Complexity of the response and dominance of nested epitopes due to recruitment of multiple T cell clones. *J Clin Invest* 92:2633–2643.
28. Inoges S, *et al.* (1999) Cytokine flow cytometry differentiates the clinical status of multiple sclerosis (MS) patients. *Clin Exp Immunol* 115:521–525.
29. Ivanov II, *et al.* (2006) The orphan nuclear receptor RORgammat directs the differentiation program of proinflammatory IL-17+ T helper cells. *Cell* 126:1121–1133.
30. Mucida D, *et al.* (2007) Reciprocal TH17 and regulatory T cell differentiation mediated by retinoic acid. *Science* 317:256–260.
31. Zhou T, *et al.* (1996) Inhibition of Nur77/Nurr1 leads to inefficient clonal deletion of self-reactive T cells. *J Exp Med* 183:1879–1892.
32. Zetterstrom RH, *et al.* (1997) Dopamine neuron agenesis in Nurr1-deficient mice. *Science* 276:248–250.
33. He YW, Deftos ML, Ojala EW, Bevan MJ (1998) RORγ t, a novel isoform of an orphan receptor, negatively regulates Fas ligand expression and IL-2 production in T cells. *Immunity* 9:797–806.
34. Kurebayeshi S, *et al.* (2000) Retinoid-related orphan receptor gamma (RORgamma) is essential for lymphoid organogenesis and controls apoptosis during thymopoiesis. *Proc Natl Acad Sci USA* 97:10132–10137.
35. Eberl G, *et al.* (2004) An essential function for the nuclear receptor RORγ(t) in the generation of fetal lymphoid tissue inducer cells. *Nat Immunol* 5:64–73.
36. Bettelli E, *et al.* (2004) Loss of T-bet, but not STAT1, prevents the development of experimental autoimmune encephalomyelitis. *J Exp Med* 200:79–87.
37. Chitnis T, *et al.* (2001) Effect of targeted disruption of STAT4 and STAT6 on the induction of experimental autoimmune encephalomyelitis. *J Clin Invest* 108:739–747.
38. Bettelli E, Oukka M, Kuchroo VK (2007) T(H)-17 cells in the circle of immunity and autoimmunity. *Nat Immunol* 8:345–350.
39. Croxford JL, Miyake S, Huang YY, Shimamura M, Yamamura T (2006) Invariant V(alpha)19i T cells regulate autoimmune inflammation. *Nat Immunol* 7:987–994.

Published November 17, 2008

JEM

ARTICLE

Aire controls the differentiation program of thymic epithelial cells in the medulla for the establishment of self-tolerance

Masashi Yano,[1] Noriyuki Kuroda,[1] Hongwei Han,[1] Makiko Meguro-Horike,[1] Yumiko Nishikawa,[1] Hiroshi Kiyonari,[2] Kentaro Maemura,[3] Yuchio Yanagawa,[4] Kunihiko Obata,[5] Satoru Takahashi,[6] Tomokatsu Ikawa,[7] Rumi Satoh,[7] Hiroshi Kawamoto,[7] Yasuhiro Mouri,[1] and Mitsuru Matsumoto[1]

[1]Division of Molecular Immunology, Institute for Enzyme Research, University of Tokushima, Tokushima 770-8503, Japan
[2]Laboratory for Animal Resources and Genetic Engineering, Center for Developmental Biology, Institute of Physical and Chemical Research (RIKEN) Kobe, Kobe 650-0047, Japan
[3]Department of Anatomy and Cell Biology, Division of Basic Medicine I, Osaka Medical College, Osaka, 569-8686, Japan
[4]Department of Genetic and Behavioral Neuroscience, Gunma University Graduate School of Medicine, Maebashi 371-8511, Japan
[5]Neuronal Circuit Mechanisms Research Group, RIKEN Brain Science Institute, Saitama 351-0198, Japan
[6]Institute of Basic Medical Sciences and Laboratory Animal Resource Center, Center for Tsukuba Advanced Research Alliance, University of Tsukuba, Tsukuba 305-8575, Japan
[7]Laboratory for Lymphocyte Development, RIKEN Research Center for Allergy and Immunology, Kanagawa 230-0045, Japan

The roles of autoimmune regulator (Aire) in the expression of the diverse arrays of tissue-restricted antigen (TRA) genes from thymic epithelial cells in the medulla (medullary thymic epithelial cells [mTECs]) and in organization of the thymic microenvironment are enigmatic. We approached this issue by creating a mouse strain in which the coding sequence of green fluorescent protein (GFP) was inserted into the *Aire* locus in a manner allowing concomitant disruption of functional Aire protein expression. We found that Aire$^+$ (i.e., GFP$^+$) mTECs were the major cell types responsible for the expression of Aire-dependent TRA genes such as *insulin 2* and *salivary protein 1*, whereas Aire-independent TRA genes such as *C-reactive protein* and *glutamate decarboxylase 67* were expressed from both Aire$^+$ and Aire$^-$ mTECs. Remarkably, absence of Aire from mTECs caused morphological changes together with altered distribution of mTECs committed to Aire expression. Furthermore, we found that the numbers of mTECs that express involucrin, a marker for terminal epidermal differentiation, were reduced in Aire-deficient mouse thymus, which was associated with nearly an absence of Hassall's corpuscle-like structures in the medulla. Our results suggest that Aire controls the differentiation program of mTECs, thereby organizing the global mTEC integrity that enables TRA expression from terminally differentiated mTECs in the thymic microenvironment.

CORRESPONDENCE
Mitsuru Matsumoto:
mitsuru@ier.tokushima-u.ac.jp

Abbreviations used: Ab, antibody; Ag, antigen; Aire, autoimmune regulator; APECED, autoimmune-polyendocrinopathy-candidiasis ectodermal dystrophy; CRP, C-reactive protein; EpCAM, epithelial cell adhesion molecule 1; FSC, forward scatter; GAD67, glutamate decarboxylase 67; K5, keratin 5; mTEC, medullary thymic epithelial cell; SAP1, salivary protein 1; SSC, side scatter; TRA, tissue-restricted Ag; UEA-1, *Ulex europaeus* agglutinin 1.

Autoimmune diseases are mediated by sustained adaptive immune responses specific for self-antigens (Ags) through unknown pathogenic mechanisms. Although breakdown of self-tolerance is considered to be the key event in the disease process, the mechanisms that allow the production of autoantibodies and/or autoreactive lymphocytes are largely enigmatic (1). Autoimmune-polyendocrinopathy-candidiasis ectodermal dystrophy (APECED; OMIM 240300) is a rather rare autoimmune disease affecting mainly the endocrine glands. Because mutation of a single gene, *autoimmune regulator* (*AIRE*), is solely responsible for the development of APECED, understanding the relationship between *AIRE* gene malfunction and the breakdown of self-tolerance promises to help unravel

The online version of this article contains supplemental material.

The Rockefeller University Press $30.00
J. Exp. Med. Vol. 205 No. 12 2827-2838
www.jem.org/cgi/doi/10.1084/jem.20080046

Supplemental Material can be found at:
http://jem.rupress.org/cgi/content/full/jem.20080046/DC1

the pathogenesis of not only APECED but also other types of autoimmune diseases (2, 3).

One of the most important aspects of AIRE in the context of autoimmunity is its limited tissue expression in medullary thymic epithelial cells (mTEC) (4, 5). mTECs are believed to play major roles in the establishment of self-tolerance by eliminating autoreactive T cells (negative selection) and/or by producing immunoregulatory T cells, which together prevent $CD4^+$ T cell–mediated organ-specific autoimmune diseases (6, 7). For this purpose, mTECs appear to express a set of self-Ags encompassing many or most of the self-Ags expressed by parenchymal organs. Supporting this hypothesis, analysis of gene expression in the thymic stroma has demonstrated that mTECs are a specialized cell type in which promiscuous expression of a broad range of peripheral tissue-restricted Ag (TRA) genes (i.e., promiscuous gene expression) is an autonomous property (8). Aire in mTECs has been suggested to regulate this promiscuous gene expression (9–11) through as yet undetermined mechanisms.

From a mechanistic viewpoint, there are two possible models to explain the function of Aire in the thymic organogenesis required for the establishment of self-tolerance. First, Aire may play a tolerogenic role within the types of mTECs characterized by Aire expression. In other words, the presence of Aire within cells is necessary in order for them to function normally as tolerance-establishing cells. Consistent with this idea, the current prevailing view on the roles of Aire in establishing self-tolerance is that Aire-positive cells are the major cell types that show promiscuous gene expression and that the lack of Aire protein within cells impairs their tolerogenic function because of the reduced transcription of TRA genes, although the developmental process of mTECs is otherwise unaltered in the absence of Aire (model 1). The second model hypothesizes that Aire is necessary for the developmental program of mTECs, including Aire-positive cells themselves. In this case, we assume that what are called Aire-positive mTECs and other Aire-dependent cell-types do not develop normally in the absence of Aire. Given that acquisition of the properties of promiscuous gene expression depends on the maturation status of mTECs (see Results and Discussion), impaired promiscuous gene expression from Aire-deficient mice can be associated with a defect of such an Aire-dependent developmental program in mTECs (model 2). Although it is still controversial whether reduced transcription of particular TRA genes in Aire-deficient mTECs can account for the development of autoimmunity targeting the corresponding self-Ags in Aire-deficient mice by itself (11–15), it is critical to determine which model provides a more appropriate explanation of Aire-dependent promiscuous gene expression to further elucidate the molecular aspects of Aire (16). Model 1 would direct research toward the mechanisms underlying how a single *Aire* gene can regulate a large number of target genes (i.e., TRA genes), whereas model 2 would accelerate studies of the developmental program of mTECs in which Aire plays a pivotal role. These two models can be tested if we can monitor the developmental process of mTECs committed to Aire expression in both the presence and absence of functional Aire protein.

This issue regarding the roles of Aire in thymic organogenesis is also directly linked to the fundamental question of how mTECs acquire their unique ability to express a broad range of self-Ags (i.e., promiscuous gene expression). The terminal differentiation model assumes that mTECs eventually acquire the capacity for promiscuous gene expression by becoming differentiated, more mature, and more promiscuous (7, 10). This model suggests that mTECs, especially Aire-positive cells, are specialized cell types that have acquired this ability through differentiation. In this context, it is noteworthy that the transcriptional machinery necessary for promiscuous gene expression other than Aire protein is considered to be acquired by mTECs independent of Aire expression in this model. The model suggests that the transcriptional unit for promiscuous gene expression becomes fully active when Aire starts to be expressed in terminally differentiated mTECs. In contrast, the developmental model considers that promiscuous gene expression is a reflection of the multipotency of immature mTECs before the developmental fate of particular cell types is determined (17). In this model, expression of a broad spectrum of TRA genes is regulated by conserved developmental programs that are active in developing mTECs, and Aire and/or $Aire^+$ cells control this process (18). Accordingly, the developmental model considers that Aire acts at the early developmental stage of mTEC differentiation, which is in marked contrast to the timing of Aire expression proposed in the terminal differentiation model. Thus, the terminal differentiation model and the developmental model favor models 1 and 2, respectively, proposed for the roles of Aire in promiscuous gene expression and self-tolerance (19).

To investigate in more detail the roles of Aire in thymic organogenesis, we have used a knock-in mouse strategy in which the coding sequence of GFP was inserted into the *Aire* gene locus in a manner allowing concomitant disruption of functional Aire protein expression. This strategy allowed us to distinguish mTECs committed to expressing Aire from Aire-nonexpressing mTECs, in both the presence and absence of functional Aire protein. In addition, with the use of knock-in mice in which thymic TRA (i.e., *glutamate decarboxylase 67* [*GAD67*]) expression can be monitored by GFP expression we also examined the cell types of mTECs responsible for promiscuous gene expression in situ. The results suggest that Aire promotes the differentiation program of mTECs and that promiscuous gene expression is accomplished in terminally differentiated mTECs that have fully matured in the presence of Aire protein.

RESULTS

Establishment of Aire/GFP knock-in mice

To examine the molecular and cellular contribution of Aire to thymic organogenesis, we established Aire/GFP knock-in mice in which expression of the GFP gene is under the transcriptional control of the endogenous *Aire* gene. In this strategy, modification of the *Aire* gene locus was minimized by inserting a GFP-neomycin resistance (neo^r) gene cassette (gfp-neo) (20) between exon 1 and exon 2 (Fig. 1 A). After

Published November 17, 2008

establishing *Aire*$^{+/gfp\text{-}neo}$ mice, they were crossed with a general deleter Cre recombinase-expressing transgenic line (21) to remove the neo^r gene cassette, which contains the herpes simplex virus *thymidine kinase* gene promoter for efficient neo^r gene expression. After confirming the removal of the neo^r gene cassette (Fig. 1 B), mice were crossed with C57BL/6 mice to select a line containing the GFP knock-in allele but not the Cre recombinase-expressing transgenic allele. *Aire*$^{+/gfp}$ mice were then crossed to obtain *Aire*$^{gfp/gfp}$ mice, which have a null mutation for the *Aire* gene because of disruption of the *Aire* gene by insertion of the GFP gene (Fig. 1 B). As expected, *Aire*$^{gfp/gfp}$ mice, but not *Aire*$^{+/gfp}$ mice, showed no expression of endogenous Aire in the thymus, as detected with polyclonal anti-Aire antibody (Ab) recognizing peptides located within the proline-rich region of Aire (unpublished data).

Using immunohistochemistry, we first examined whether GFP expression from *Aire*$^{+/gfp}$ mouse thymus reflects endogenous *Aire* gene expression. Stromal cells showing variable extents of GFP expression in the cytoplasm and nucleus were scattered throughout the thymic medulla (Fig. 1 C). The medullary region was identified by staining with *Ulex europaeus* agglutinin 1 (UEA-1) (Fig. 2 A), anti–epithelial cell adhesion molecule 1 (EpCAM) mAb (Fig. 2 B), or anti–keratin 5 (K5) Ab (Fig. S1 A, available at http://www.jem.org/cgi/content/full/jem.20080046/DC1). GFP-expressing cells from *Aire*$^{+/gfp}$ mouse thymus showed a dendritic to fibroblastic morphology and were enriched at the cortico-medullary junction (Fig. 1 C; Fig. 2, A and B; and Fig. S1 A). When doubly stained with anti-Aire Ab, most of the GFP-expressing cells contained variable amounts of Aire nuclear dots within their nuclei (Fig. 1 C), indicating that GFP expression is under the transcriptional control of the authentic *Aire* gene. However, a few cells showed Aire nuclear dots without any detectable GFP expression (Fig. 1 C, arrows) or expressed GFP without obvious Aire nuclear dots (not depicted). As expected, *Aire*$^{+/+}$ mouse thymus showed no GFP signals (Fig. 2, A and B). Notably, most of the CD11c-positive DCs in the thymus were GFP negative (Fig. S1 B), suggesting that Aire expression from thymic DCs is negligible compared with that from mTECs.

Altered thymic organization in Aire-deficient mice

We then examined the effect of Aire deficiency on thymic organization in *Aire*$^{gfp/gfp}$ mouse thymus sections, focusing on the production of cells genetically marked with GFP and, therefore, active in *Aire* gene transcription but lacking functional Aire protein. There were many GFP$^+$ "Aire-less" TECs within the medulla (Figs. 2, A and B; and Fig. S1 A), indicating clearly that Aire protein itself is not necessary for the production of particular mTEC lineages committed to express Aire. However, detailed inspection demonstrated that the morphology and location of GFP$^+$ cells from *Aire*$^{gfp/gfp}$ thymus were altered compared with those of GFP$^+$ cells containing functional Aire protein from *Aire*$^{+/gfp}$ mouse thymus. First, we noticed that the cell shape of GFP$^+$ mTECs lacking functional Aire protein was altered; in *Aire*$^{gfp/gfp}$ thymus, more GFP$^+$ cells exhibited a globular shape instead of a dendritic to fibroblastic morphology, compared with *Aire*$^{+/gfp}$ thymus (Fig. 2 C, arrows). The lower preponderance of a dendritic shape of GFP$^+$ Aire-less mTECs was verified by statistical analysis. We calculated the level of cell shape complexity for each GFP$^+$ cell by dividing the length of the cellular periphery by the cell area using a computer program (i.e., the higher

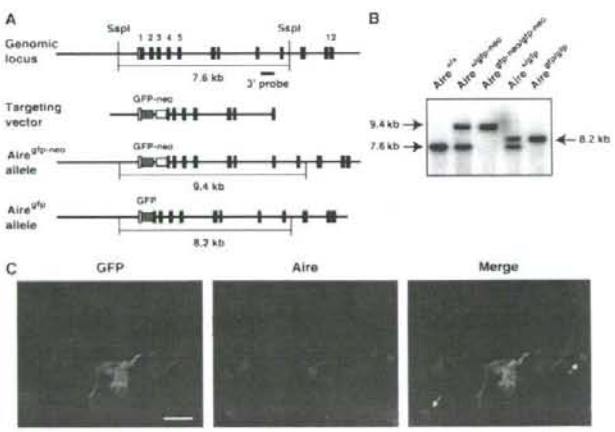

Figure 1. Establishment of Aire/GFP knock-in mice. (A) Targeted insertion of the GFP gene into the *Aire* gene locus by homologous recombination. SspI, *SspI* restriction site. (B) Southern blot analysis of genomic DNA from offspring of Aire/GFP knock-in mice. Tail DNA was digested with *SspI* and hybridized with the 3′ probe shown in A. (C) Concomitant expression of GFP (green) and endogenous mouse Aire (red) assessed by immunohistochemistry of a thymus section from an *Aire*$^{+/gfp}$ mouse. Cells positive for Aire staining but negative for GFP expression are marked with arrows. Bar, 20 μm. One representative experiment from a total of four repeats is shown.

the value, the more complex the cell shape). GFP$^+$ cells from *Aire*$^{gfp/gfp}$ thymus showed lower values (i.e., less complexity per cell) and a narrower distribution of values (i.e., less heterogeneity of cell shape) than those from *Aire*$^{+/gfp}$ thymus (Fig. 2 D). Because a gene-dosage effect has been noticed at the *Aire* gene locus (11), we carefully excluded the possibility that the altered shape of GFP$^+$ cells from *Aire*$^{gfp/gfp}$ thymus was due simply to higher GFP protein expression within each cell, i.e., imposing a potentially toxic burden on the cells. For this purpose, we crossed *Aire*$^{+/gfp}$ mice with *Aire*$^{-/-}$ mice (12) to establish *Aire*$^{-/gfp}$ mice in which the *gfp* allele is single, as in *Aire*$^{+/gfp}$ mice (Fig. S2 A). Similarly to the *Aire*$^{gfp/gfp}$ thymus analysis, GFP$^+$ cells from *Aire*$^{-/gfp}$ thymus demonstrated less complexity of cell shape than those from *Aire*$^{+/gfp}$ thymus, as confirmed using the same method of statistical analysis (Fig. S2 B).

Although we analyzed the thymic organization of *Aire*$^{gfp/gfp}$ mice before the onset of autoimmune pathology (i.e., 4–6 wk after birth), we also excluded the possibility that the altered cell shape of GFP$^+$ cells from *Aire*$^{gfp/gfp}$ thymus was secondary to the autoimmune phenotypes by establishing *Aire*$^{-/gfp}$ mice expressing the OT-II TCR transgene in which the autoreactive T cell repertoire is absent (Fig. S3 A). Morphological changes in GFP$^+$ cells were similarly observed in these mice (Fig. S3 B), suggesting that the altered shape of GFP$^+$ cells lacking Aire protein was independent of autoimmune phenotype.

Second, we noticed that the distribution pattern of mTECs committed to Aire expression was also affected in the absence of functional Aire protein. In contrast with the enrichment of GFP$^+$ cells from *Aire*$^{+/gfp}$ thymus at the cortico-medullary junction, GFP$^+$ cells from *Aire*$^{gfp/gfp}$ thymus tended to be localized

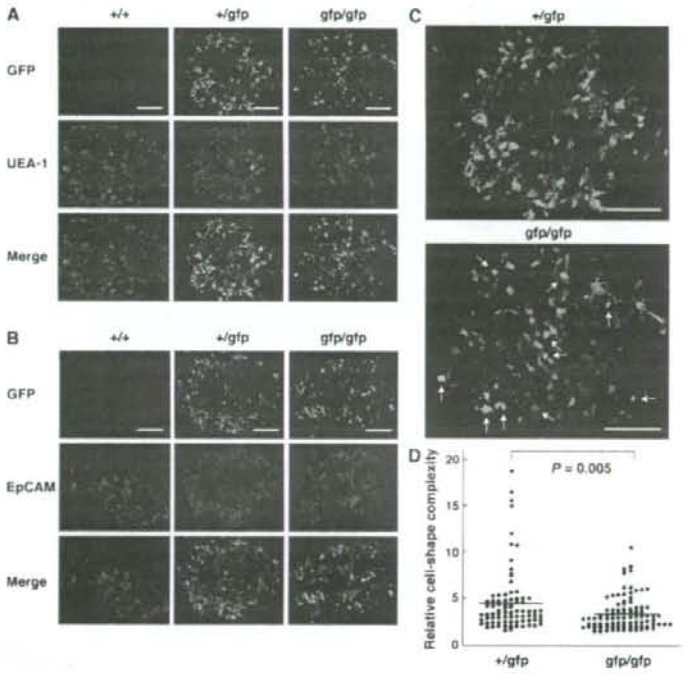

Figure 2. Altered morphology and distribution of mTECs committed to express Aire in the absence of functional Aire protein. (A and B) mTECs active in *Aire* gene transcription were visualized by immunohistochemistry with anti-GFP Ab (green). The medullary region was identified by staining with UEA-1 (A) or anti-EpCAM mAb (B; red). Bars, 100 µm. One representative experiment from a total of five repeats is shown. (C) Enlargement of the staining with anti-GFP Ab from A for demonstration of altered morphology and distribution of mTECs committed to express Aire in *Aire*$^{gfp/gfp}$ mouse thymus. There were more GFP$^+$ cells with globular shapes (bottom, arrows) in *Aire*$^{gfp/gfp}$ thymus than in *Aire*$^{+/gfp}$ thymus. GFP$^+$ cells from *Aire*$^{-/gfp}$ thymus were enriched at the cortico-medullary junction (top), whereas GFP$^+$ cells from *Aire*$^{gfp/gfp}$ thymus tended to be localized more evenly within each medulla or even enriched at the center of the medulla (bottom). Bars, 100 µm. One representative experiment from a total of five repeats is shown. (D) Morphological changes in the shape of GFP$^+$ cells from *Aire*$^{gfp/gfp}$ mouse thymus demonstrated in C were analyzed statistically. Each circle corresponds to the relative cell shape complexity of a single GFP$^+$ cell calculated with a computer program (see Materials and methods). A total of 80 and 88 GFP$^+$ cells from *Aire*$^{+/gfp}$ and *Aire*$^{gfp/gfp}$ thymi, respectively, were evaluated. Red lines represent mean values. Two mice for each group were analyzed, and similar results were obtained from a total of three repeats.

Published November 17, 2008

more uniformly within each medulla or even enriched at the medulla center (Fig. 2 C and Fig. S1 A). Altered distribution of GFP$^+$ Aire-less mTECs was also evident in *Aire*$^{-/gfp}$ mice (Fig. S2 A), as well as in *Aire*$^{-/gfp}$ mice expressing the nonautoreactive OT-II TCR transgene (Fig. S3 A). Collectively, production of a particular mTEC lineage committed to express Aire is not determined by Aire protein alone. However, Aire deficiency in these cells results in morphological changes together with altered location within the medulla, suggesting a role of Aire in the differentiation program of mTECs in a cell-intrinsic manner.

Analysis of embryonic thymus demonstrated that GFP$^+$ cells were absent at embryonic day 13.5, but clearly present at embryonic day 16.5 in both *Aire*$^{+/gfp}$ and *Aire*$^{gfp/gfp}$ mice (Fig. S1 C). Although the effect of absence of Aire protein on the location of GFP$^+$ cells from *Aire*$^{gfp/gfp}$ mice at the embryonic and early P1 (postneonatal) stages was difficult to evaluate because of the less organized thymic structure together with relatively small numbers of GFP$^+$ cells at those stages, morphological alteration of each mTEC committed to Aire expression was already evident at the neonatal stage (P1; Fig. S4 A), as confirmed by the same statistical analysis applied to Fig. 2 D (Fig. S4 B). The properties of GFP$^-$ (i.e., Aire nonexpressing) mTECs as evaluated by immunohistochemistry with UEA-1, anti-EpCAM Ab (Fig. 2, A and B), anti-K5 Ab (Fig. S1 A), ER-TR5 Ab, anti-claudin 3/4 Abs, and MTS10 Ab (not depicted) showed no obvious difference between *Aire*$^{+/gfp}$ and *Aire*$^{gfp/gfp}$ adult thymi.

In addition to the histological evaluation of mTECs based on Aire/GFP expression, another possibility that Aire controls the differentiation program of mTECs has emerged from studies focusing on the cell differentiation markers expressed by mTECs. In the skin, involucrin expression is restricted to postmitotic epithelial cells and serves as a marker of epidermal and follicular terminal differentiation (22). Interestingly, immunohistochemistry of the human thymus using anti-involucrin Ab stains characteristic swirled epithelial structures known as Hassall's corpuscles (23), which is consistent with the fact that Hassall's corpuscles are composed of terminally differentiated mTECs (24). When thymus sections from Aire-sufficient mice were stained with anti-involucrin Ab, involucrin-expressing cells were scattered within the EpCAM$^+$ thymic medulla (Fig. 3 A). The number of involucrin-expressing cells was age dependent and declined between 8 and 11 wk (Fig. 3 B and Table S1, available at http://www.jem.org/cgi/content/full/jem.20080046/DC1). In addition, we occasionally found larger involucrin-expressing structures with a hyalinized degenerated core in the thymic medulla from Aire-sufficient mice, which is reminiscent of Hassall's corpuscles in human thymus (Fig. 3 C). Remarkably, the numbers of mTECs expressing involucrin in Aire-deficient mice were significantly lower than those in Aire-sufficient mice, especially at 4 and 8 wk of age (Fig. 3 B). Furthermore, we observed no typical Hassall's corpuscle-like structures in the thymus of Aire-deficient mice at any age, which is in contrast to those seen in Aire-sufficient mice (Table S1). These results further support the notion that lack of Aire in mTECs alters their differentiation program, thereby altering mTEC integrity.

Next, we used flow cytometric analysis to examine GFP-expressing cells from the thymus. Thymic stromal cells were released enzymatically from adult thymi and stained with anti-CD45 mAb and UEA-1, together with anti-CD80 and anti–MHC class II mAbs. *Aire*$^{+/gfp}$ thymus contained 4.5% UEA-1$^+$GFP$^+$ (i.e., Aire$^+$) cells (from here on simply designated GFP$^+$ cells) in the population of CD45$^-$ stromal cells (Fig. 4 A). When forward scatter (FSC) and side scatter (SSC) parameters were compared between GFP$^+$ cells and UEA-1$^+$GFP$^-$ cells (from here on simply designated GFP$^-$ cells), GFP$^+$ cells were larger and more broadly distributed compared with GFP$^-$ cells (Fig. 4 B, left), suggesting a distinct cellular morphology of Aire$^+$ cells among mTECs. *Aire*$^{gfp/gfp}$ thymus also contained GFP$^+$ cells in the population of CD45$^-$ stromal cells (Fig. 4 A), as already observed by immunohistochemical analysis (Figs. 2 and S1). Interestingly, the proportion of GFP$^+$ cells in *Aire*$^{gfp/gfp}$ thymus was consistently

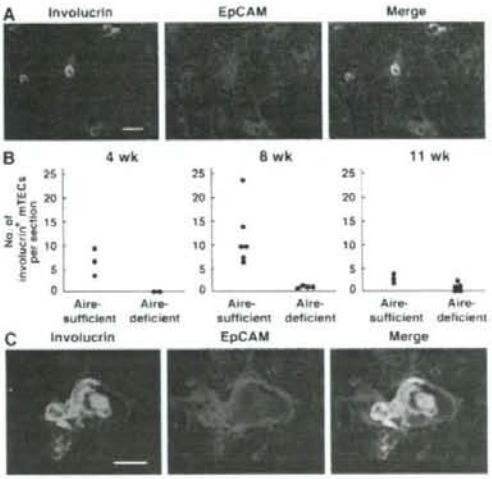

Figure 3. Reduced numbers of terminally differentiated mTECs in the absence of Aire. (A) Involucrin-expressing mTECs (green) were scattered within the thymic medulla (red; stained with anti-EpCAM Ab) of Aire-sufficient mice. Bar, 50 µm. (B) Numbers of involucrin-expressing mTECs were reduced in Aire-deficient mice at 4 (left) and 8 (middle) wk of age. Numbers of involucrin-expressing mTECs in Aire-sufficient mice declined at 11 wk of age (right). Each circle corresponds to the mean number of involucrin-expressing mTECs per section examined in individual mice. Detailed information for the mice examined from a total of five experiments is presented in Table S1 (available at http://www.jem.org/cgi/content/full/jem.20080046/DC1). (C) Hassall's corpuscle-like structures seen in Aire-sufficient mouse thymus stained with anti-involucrin Ab (green) together with anti-EpCAM Ab (red). These discrete and larger involucrin-expressing structures were scarcely detectable in Aire-deficient mouse thymus. Bar, 20 µm. One representative experiment from a total of five repeats is shown.

Published November 17, 2008

30–40% higher than in *Aire*$^{+/gfp}$ thymus (Fig. 4 A). Consequently, the ratio of GFP$^+$ cells to GFP$^-$ cells was higher in *Aire*$^{gfp/gfp}$ thymus (~1:5) compared with that in *Aire*$^{+/gfp}$ thymus (~1:10). Although the difference in FSC/SSC parameters between GFP$^+$ and GFP$^-$ cells observed for *Aire*$^{+/gfp}$ mice was also seen in *Aire*$^{gfp/gfp}$ mice (Fig. 4 B, right), FSC/SSC plots of GFP$^+$ cells from *Aire*$^{gfp/gfp}$ mice showed a more condensed profile over a narrower region compared with GFP$^+$ cells from *Aire*$^{+/gfp}$ mice (Fig. 4 B, top), which might reflect the morphological changes in GFP$^+$ mTECs observed by immunohistochemistry (Fig. 2 C). We recorded no GFP expression from CD45$^+$ hematopoietic cells (not depicted) or from CD45$^-$UEA-1$^-$ thymic stromal cells from either *Aire*$^{+/gfp}$ or *Aire*$^{gfp/gfp}$ mice (Fig. 4 A).

We then analyzed the expression of CD80 and MHC class II from each of the populations separated on the basis of GFP expression and UEA-1 binding. GFP$^+$ cells from *Aire*$^{+/gfp}$ mice expressed both CD80 and MHC class II at high levels (CD80^{hi}/class II^{hi}), whereas GFP$^-$ cells from the same animals expressed intermediate to low levels of both CD80 and MHC class II (Fig. 4 C, left). GFP$^+$ cells from *Aire*$^{gfp/gfp}$ thymus were also CD80^{hi}/class II^{hi} (Fig. 4 C, right), indicating that expression of these Ag presentation-related molecules was Aire independent. Indeed, expression levels of both CD80 and MHC class II from GFP$^+$ cells were almost indistinguishable between *Aire*$^{+/gfp}$ and *Aire*$^{gfp/gfp}$ mice when the two flow cytometric profiles were merged (Fig. 4 D, left). However, although difference was small, expression of both CD80 and MHC class II from GFP$^-$ cells from *Aire*$^{gfp/gfp}$ mice was consistently lower than that from *Aire*$^{+/gfp}$ mice (Fig. 4 D, right). This result may indicate that the absence of normal Aire-expressing cells from the medulla is accompanied by phenotypic alteration of Aire-nonexpressing mTECs, which was not evident with the immunohistochemical analysis with the commonly used medullary epithelial cell markers (Fig. 2, A and B; and Fig. S1 A). Collectively, the results suggest that *Aire* deficiency results in a global alteration of the thymic microenvironment that involves not only mTECs committed to express Aire but also the Aire-nonexpressing mTECs that surround Aire$^+$ cells.

Aire-dependent TRA gene expression

Although Aire has been suggested to regulate promiscuous gene expression in mTECs (9, 10), demonstration that Aire$^+$ cells are the major source of promiscuous gene expression from mTECs is still incomplete in the absence of appropriate cell markers for Aire-expressing cell lineages. Existing data for promiscuous gene expression from mTECs were obtained

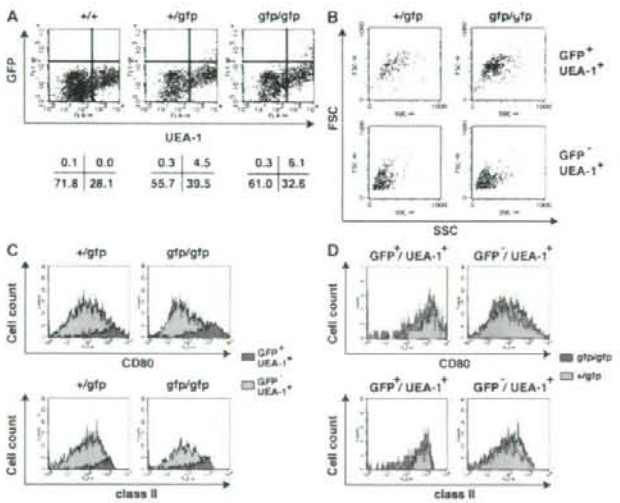

Figure 4. Global alteration of mTEC phenotypes in the absence of Aire. (A) Detection of GFP-expressing cells from thymic stroma by flow cytometric analysis. CD45$^-$ thymic stromal cells were analyzed for the expression of GFP together with binding of UEA-1. Percentages of cells from each fraction are indicated below. (B) mTECs committed to express Aire were larger than mTECs noncommitted to express Aire, irrespective of the presence of Aire protein. FSC/SSC profiles of mTECs committed to express Aire were altered in the absence of functional Aire protein (top). Each FSC/SSC profile was obtained by back gating the corresponding fractions from A based on the expression of GFP and UEA-1. (C) CD80 and MHC class II expression levels were higher in mTECs committed to express Aire than in mTECs noncommitted to express Aire, irrespective of the presence of functional Aire protein. Filled profiles in green and gray are from GFP$^+$ and GFP$^-$ mTECs, respectively. (D) CD80 and MHC class II expression from mTECs committed to express Aire were indistinguishable between *Aire*$^{+/gfp}$ and *Aire*$^{gfp/gfp}$ mice (left) but were reduced in mTECs noncommitted to express Aire in the absence of functional Aire protein (right). Filled profiles in gray and green lines are from *Aire*$^{+/gfp}$ and *Aire*$^{gfp/gfp}$ mice, respectively. Flow cytometric profiles from C were merged for comparison. One representative result from a total of more than five repeats is shown.

Published November 17, 2008

by flow cytometric sorting using surrogate Aire$^+$ cell markers such as CD80 and MHC class II. As a result, it is not yet clear which population of mTECs (i.e., Aire-expressing or Aire-nonexpressing mTECs) is deficient in promiscuous gene expression as a result of absence of functional Aire protein. To answer this question, we separated GFP$^+$ and GFP$^-$ mTECs from both *Aire*$^{+/gfp}$ and *Aire*$^{gfp/gfp}$ mice and examined the expression of several TRA genes, including both Aire-dependent (i.e., *insulin 2* and *salivary protein 1* [*SAP1*]) and Aire-independent (*C-reactive protein* [*CRP*]) TRA genes; expression of the former and the latter gene classes has been demonstrated to be reduced or unchanged, respectively, in CD80^{hi}/class II^{hi} Aire-deficient mTECs (9, 10). GFP$^+$ mTECs from *Aire*$^{+/gfp}$ mice showed the highest expression of *insulin 2* and *SAP1*, and expression of those genes was much lower in GFP$^-$ mTECs from the same animals (Fig. 5). Remarkably, both GFP$^+$ and GFP$^-$ mTECs from *Aire*$^{gfp/gfp}$ mice expressed almost none of the Aire-dependent TRA genes *insulin 2* and *SAP1*. mTECs defined by UEA-1 binding from *Aire*$^{+/+}$ mice, which includes both Aire$^+$ and Aire$^-$ cells, showed intermediate expression of those genes. These results clearly indicate two important features of promiscuous gene expression in mTECs. First, Aire$^+$ mTECs are the major cell types responsible for the expression of Aire-dependent TRA genes. Second, mTECs cannot express Aire-dependent TRA genes in the absence of functional Aire protein, even though the lineage commitment to express Aire and the expression of Ag presentation-related molecules, such as CD80 and MHC class II, are preserved (Fig. 4 C). It is important to emphasize that the latter observation does not necessarily mean that Aire acts on the already existing transcriptional machinery required for TRA gene expression within established terminally differentiated mTECs. Rather, in the light of the fact that GFP$^+$ Aire-less mTECs show defective development, as indicated by their altered morphology and distribution, we suggest that Aire$^+$ mTECs acquire their unique machinery for promiscuous gene expression only when they have fully achieved maturation with the help of Aire protein (see Discussion and see Fig. 8).

In marked contrast to Aire-dependent TRA genes, expression of an Aire-independent TRA gene, *CRP*, from GFP$^+$ mTECs was indistinguishable between *Aire*$^{+/gfp}$ and *Aire*$^{gfp/gfp}$ mice. *CRP* expression from GFP$^-$ mTECs was detectable, although the levels were lower than from GFP$^+$ mTECs, and was also similar between *Aire*$^{+/gfp}$ and *Aire*$^{gfp/gfp}$ mice (Fig. 5). As expected, the *Aire* gene was highly expressed from GFP$^+$ mTECs of *Aire*$^{+/gfp}$ mice, although a low level of *Aire* gene expression was detected from GFP$^-$ mTECs, which is possibly a result of slight contamination by cells expressing a trace amount of GFP (i.e., Aire) in this fraction. Expression of the *Aire* gene from both GFP$^+$ and GFP$^-$ cells of *Aire*$^{gfp/gfp}$ mice was at background levels.

Aire-independent TRA gene expression in situ from mTECs

The results in the previous section suggest that individual mTECs do not express a broad array of TRA genes. Rather, each mTEC seems to express a different spectrum of TRA genes. Some TRA genes, such as *insulin 2* and *SAP1* (previously recognized as Aire-dependent genes; references 9, 10), were predominantly expressed from cells of the Aire$^+$ mTEC lineage only when Aire protein was present within the cells, and other TRA genes, such as *CRP* (previously recognized as an Aire-independent gene; references 9, 10), were expressed from both Aire$^+$ and Aire$^-$ mTECs irrespective of the presence of Aire protein. The latter situation was further investigated with the use of GAD67/GFP knock-in mice (*GAD67*$^{+/gfp}$ mice). *GAD67*, an Aire-independent TRA gene that is expressed in the brain and pancreas, is

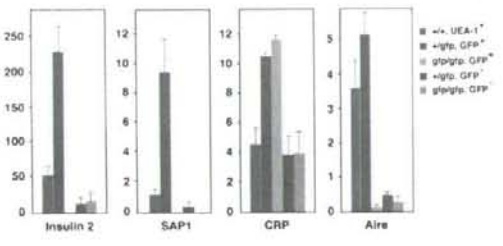

Figure 5. TRA gene expression from mTECs assessed by real-time PCR. Expression of *insulin 2*, *SAP1*, *CRP*, and *Aire* was examined from each fraction of mTECs sorted on the basis of the flow cytometric profile demonstrated in Fig. 4 A. Color bars corresponding to each fraction are indicated on the right. Aire$^+$ mTECs were the major cell types responsible for the expression of Aire-dependent TRA genes (*insulin 2* and *SAP1*), whereas an Aire-independent TRA gene (*CRP*) was expressed from both Aire$^+$ and Aire$^-$ mTECs. Aire expression was assessed to verify the proper sorting of each mTEC fraction. Numbers are relative gene expression level compared with that of the *Hprt* gene. Results are expressed as the mean ± SEM for triplicate wells of one representative experiment from a total of three repeat experiments.

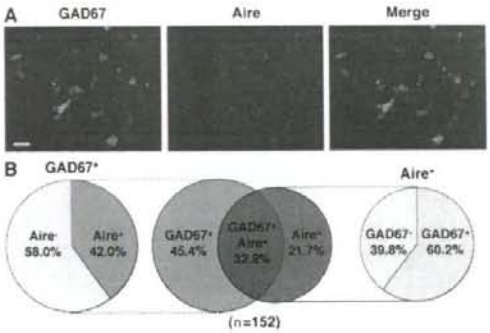

Figure 6. Expression of the Aire-independent TRA gene *GAD67* and of Aire from mTECs in situ. (A) Expression of the *GAD67* gene and Aire was detected by immunohistochemistry with anti-GFP Ab (green) and anti-Aire Ab (red), respectively, in thymus sections from GAD67/GFP knock-in mice. Bar, 20 µm. (B) Results obtained as described for A were calculated for a total of 152 mTECs expressing the *GAD67* gene and/or Aire. One representative experiment from a total of three repeats is shown.

also active in mTECs from *GAD67*$^{+/gfp}$ mice (25). Using immunohistochemistry, we examined the expression of GAD67 together with Aire in *GAD67*$^{+/gfp}$ mouse thymus sections. There were three types of TECs: GAD67$^+$Aire$^-$ (45.4%), GAD67$^+$Aire$^+$ (32.9%), and GAD67$^-$Aire$^+$ (21.7%) (Fig. 6, A and B). Among the GAD67$^+$ mTECs, 42.0% expressed Aire and the rest did not (Fig. 6 B), consistent with the Aire-independent nature of *GAD67* gene expression (9, 10). Conversely, among the Aire$^+$ mTECs, 60.2% expressed GAD67 and the rest did not, suggesting that Aire expression is not sufficient for TRA expression, at least for this Aire-independent TRA gene.

Expression of *Aire* and Aire-independent TRA genes by nonproliferating mTECs

Previous studies suggested that Aire is predominantly expressed by terminally differentiated cells on the basis of their poor incorporation of BrdU (26, 27). We confirmed this finding by injecting BrdU into *Aire*$^{+/gfp}$ mice. BrdU incorporation was scarce in GFP$^+$ mTECs (Fig. 7 A, top). We similarly examined which type of mTECs, immature proliferating or mature nonproliferating, express GAD67 by injecting BrdU into GAD67/GFP knock-in mice. We found that GFP$^+$ mTECs incorporated BrdU only weakly (Fig. 7 A, bottom), suggesting that expression of this Aire-independent TRA gene is also imposed on terminally differentiated cells rather on immature proliferating mTECs.

p63 is strongly expressed in epithelial stem cells of the thymus and specifically functions to maintain their extraordinary proliferative capacity (28). To examine whether mTECs expressing the *Aire* and *GAD67* genes have this high proliferative capacity, we examined p63 expression from thymi of Aire/GFP knock-in and GAD67/GFP knock-in adult mice. mTECs expressing GFP from both mouse strains showed little p63 expression by immunohistochemistry (Fig. 7 B), suggesting that neither of these genes is expressed in mTECs with high proliferative capacity. Instead, Aire seems to function within mTECs in the later stages of differentiation, when the cells are also responsible for TRA gene expression.

DISCUSSION

In the present study, we addressed fundamental questions regarding how mTECs acquire the capacity for promiscuous gene expression with the participation of Aire, with the hope that understanding the roles of Aire in thymic organogenesis will help to unravel the molecular mechanisms responsible for expression of immunological self in the thymic microenvironment. The issues include the following: first, whether Aire itself is necessary for the production and/or differentiation

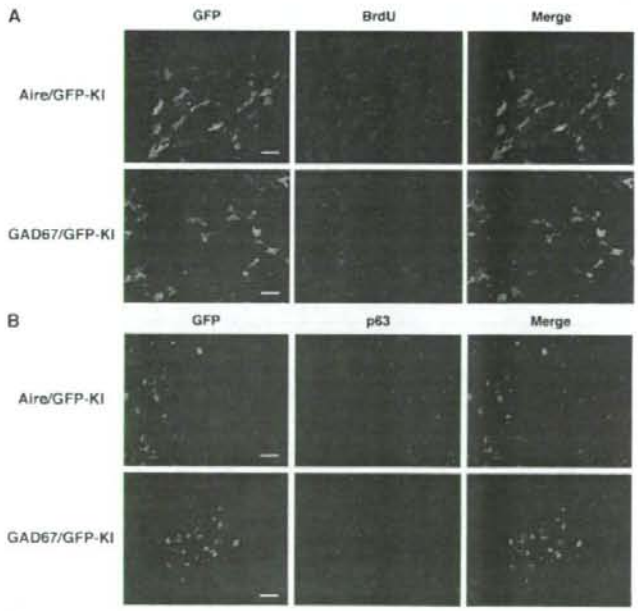

Figure 7. Expression of the *Aire* and *GAD67* genes by nonproliferating mTECs. (A) BrdU incorporation by *Aire*- and *GAD67*-expressing mTECs was evaluated 4 h after i.p. injection of BrdU into *Aire*$^{+/gfp}$ and *GAD67*$^{+/gfp}$ mice, respectively. The thymus sections were stained with anti-GFP (green) and anti-BrdU (red) Abs. Bars, 20 µm. (B) p63 (red) was not detected in mTECs expressing the *Aire* and *GAD67* genes (green). Bars, 40 µm. One representative experiment from a total of four repeats is shown.

Published November 17, 2008

program of Aire$^+$ cell lineages; second, whether Aire$^+$ mTECs are necessary for the structural and/or functional organization of other types of mTECs; third, to what extent Aire$^+$ mTECs contribute to the expression of TRA genes; and fourth, the nature of the maturation status of mTECs that express Aire and are responsible for TRA expression. Because Aire-specific Ab cannot be used to investigate the differentiation process of mTECs committed to express Aire in the absence of Aire protein, we established Aire/GFP knock-in mice in which the GFP marker gene was inserted into the *Aire* gene locus in a manner allowing concomitant disruption of functional Aire protein expression. In $Aire^{+/gfp}$ mice, this strategy also enables us to distinguish Aire-expressing cells from Aire-nonexpressing cells without introducing any cell markers incompletely unique to Aire-expressing cells. Accordingly, mTECs committed to Aire expression were faithfully GFP marked with this strategy; mTECs transcriptionally active for the *Aire* gene were mostly positive for staining with anti-Aire Ab by immunohistochemistry. There were, however, small numbers of cells that were either positive for Aire staining but negative for *Aire* gene transcription (i.e., GFP$^-$) or, conversely, positive for *Aire* gene transcription (i.e., GFP$^+$) but negative for Aire staining. The former cell type could result from different half-lives of the two proteins (GFP vs. Aire), whereas the latter cell type could result from Aire protein being present as a diffuse nucleoplasmic form (more difficult to recognize) instead of the typical nuclear-dot form (29). Alternatively, these discrepancies could simply be accounted for by differences in detection sensitivity. Indeed, RT-PCR analysis of flow cytometry–sorted cell fractions showed the expected patterns of *Aire* gene expression.

With Aire/GFP knock-in mice, we have clearly demonstrated that Aire$^+$ mTECs are the major cell types responsible for the expression of so-called Aire-dependent TRA genes such as *insulin 2* and *SAP1* (9, 10). These genes were almost exclusively expressed from GFP$^+$ mTECs of $Aire^{+/gfp}$ mice but not of $Aire^{gfp/gfp}$ mice. In contrast, expression of Aire-independent genes, such as *CRP*, was not affected by the absence of Aire. *CRP* expression from GFP$^+$ cells was similar between $Aire^{+/gfp}$ and $Aire^{gfp/gfp}$ mice. *CRP* expression, although at lower levels, was also observed from GFP$^-$ cells and, again, was indistinguishable between $Aire^{+/gfp}$ and $Aire^{gfp/gfp}$ mice. Expression of *GAD67* in an Aire-independent manner (9, 10) was also supported by immunohistochemistry of GAD67/GFP knock-in thymus, demonstrating *GAD67* expression irrespective of the presence of Aire protein in each mTEC. We speculate that the Aire dependency of TRAs reflects, in part, the cell types in which TRAs are expressed; expression of Aire-dependent genes is confined to Aire$^+$ mTECs, whereas expression of Aire-independent genes occurs from both Aire$^+$ and Aire$^-$ mTECs. It is of note that mTECs do not uniformly express the overlapping spectrum of TRAs, as exemplified by the scattered expression of the *GAD67* gene in GAD67/GFP knock-in mouse thymus. Similarly, although Aire$^+$ mTECs are the major cell types responsible for the expression of Aire-dependent TRA genes, this does not mean that all Aire$^+$ mTECs express Aire-dependent TRA genes uniformly. Indeed, single-cell analysis has demonstrated that expression of Aire in mTECs is not sufficient for simultaneous coexpression of Aire-dependent TRA genes (17). Thus, we favor the notion that promiscuous gene expression reflects the thymus-wide summation of expression of a small number of self-Ags by individual mTECs rather than expression of the complete spectrum of self-Ags by each cell (17, 18).

Because expression of transcription factors associated with developmental plasticity of progenitor cells (i.e., *Nanog*, *Oct4* and *Sox2*) is Aire-dependent in mTECs (18), the developmental model predicts that Aire acts early in the development of mTECs. The developmental model also suggests that promiscuous gene expression represents coordinated gene expression reflecting an alternate program of epithelial differentiation among actively proliferating mTECs at their progenitor or immature stages (19). However, accumulating data together with the results of the present study do not support such a view (26, 27). Rather, it is likely that Aire is acting at the late differentiation stages of mTECs. Accordingly, Aire-dependent processes for achieving promiscuous gene expression might also be active at the late differentiation stages of mTECs (see the subsequent paragraph). Clearly, this does not involve mTECs gaining the ability to express CD80 from CD80^{lo} precursors (30) because GFP$^+$ mTECs from $Aire^{gfp/gfp}$ mice demonstrated normal levels of CD80 expression. It is necessary to dissect the developmental process of mTECs, thereby precisely identifying the Aire-dependent steps of mTEC differentiation.

Given that Aire-expressing cells are terminally differentiated, the demonstration that Aire$^+$ mTECs are the major cell types responsible for expression of TRA genes, at least for Aire-dependent genes, apparently favors the terminal differentiation model for Aire-dependent promiscuous gene expression from mTECs (7, 10, 11). However, our results do support a key aspect of a role for Aire in the developmental model (17–19): absence of Aire in mTECs causes morphological changes together with altered distribution of mTECs committed to express Aire. Indeed, the difference in appearance of GFP-expressing cells was distinct enough to allow discrimination between $Aire^{+/gfp}$ and $Aire^{gfp/gfp}$ mouse sections by blind analysis. Interestingly, Gillard et al. (18) noted that globular mTECs without visible cellular projections were more prominent in Aire-deficient thymus, which could represent the GFP$^+$ globular mTECs we observed in $Aire^{gfp/gfp}$ mice. Furthermore, expression of functional molecules, such as CD80 and MHC class II from mTECs noncommitted to express Aire, was also affected by the absence of Aire, suggesting that Aire and/or Aire$^+$ mTECs influence the organization of mTECs beyond simply controlling promiscuous gene expression within Aire-expressing cell lineages. We do not believe that the demonstration that terminally differentiated Aire-expressing cells are the major source of promiscuous gene expression (apparently favoring the terminal differentiation model) and the demonstration that Aire and/or Aire$^+$ cells controls thymic organogenesis (consistent with the developmental model; reference 18 and present study) are mutually exclusive. Instead,

Aire could both promote the differentiation program of mTECs committed to express Aire, ensuring that they become fully equipped with the necessary machinery for promiscuous gene expression, and be an efficient driver of promiscuous gene expression in such cells. Thus, promiscuous gene expression seems to be accomplished in terminally differentiated mTECs that have matured in the presence of Aire protein (Fig. 8). Alternatively, Aire might be necessary for maintenance of a terminally differentiated state in which mTECs manifest a dendritic shape with fully competent promiscuous gene expression.

We found that the numbers of mTECs expressing involucrin, a marker of epidermal differentiation (22), were reduced in Aire-deficient mouse thymus. It was noteworthy that involucrin-expressing mTECs themselves were negative for Aire expression with immunohistochemistry (unpublished data), thus making it unlikely that *involucrin* gene expression in mTECs is under direct transcriptional control by Aire as a part of TRA gene expression. Similarly, it is unknown whether impaired involucrin expression is specific to mTECs committed to Aire expression or whether lack of Aire$^+$ mTECs affects the differentiation of other type(s) of mTECs that would otherwise express involucrin at their terminally differentiated stages. Based on the fact that GFP$^+$ Aire-less mTECs showed alterations in their morphology as well as distribution, we assume that the former possibility is more likely. Interestingly,

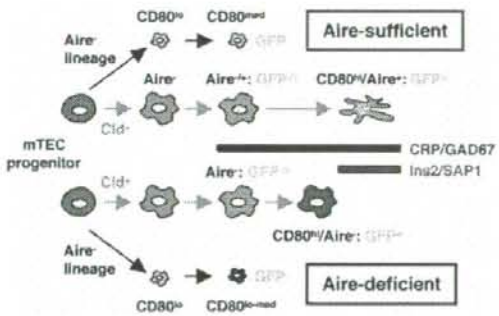

Figure 8. Schematic representation of the roles of Aire in mTEC differentiation and TRA gene expression. Aire-expressing cell lineages develop from mTEC progenitor cells through concomitant expression of claudin (26). Expression of Aire-dependent TRA genes, such as *insulin 2* and *SAP1*, can be accomplished in terminally differentiated mTECs showing a dendritic to fibroblastic morphology that have fully matured with the help of Aire protein (marked as Aire-sufficient). Lack of Aire in mTECs results in premature termination of differentiation, although claudin$^+$ Aire-expressing cell lineages can still develop and pass the CD80-expressing maturation stage (marked as Aire-deficient). These CD80^{lo} Aire-less mTECs have a more globular cell shape and lack transcriptional machinery for Aire-dependent TRA genes. Because Aire-independent TRA genes, such as *CRP* and *GAD67*, can be expressed before the terminal differentiation stages, lack of Aire has little impact on their expression. The possibility also remains that Aire is necessary for the maintenance of a terminally differentiated state, in which mTECs manifest a dendritic shape with fully competent promiscuous gene expression.

we found that reduction of involucrin-expressing mTECs in Aire-deficient mice was associated with a nearly absence of Hassall's corpuscle-like structures, although the exact relevance of this phenotype to the breakdown of central tolerance in Aire-deficient mice remains unknown (31). Together with the fact that formation of thymic cysts is a predominant feature of Aire-deficient mice (18, 26), it seems likely that Aire exerts more global control of the differentiation program of mTECs than was initially thought.

Finally, although we have demonstrated that Aire organizes the global mTEC integrity that facilitates promiscuous gene expression in the thymic microenvironment, the exact nature of the mTEC differentiation program under the control of Aire protein still remains unknown. We have demonstrated that both *Aire* and an Aire-independent TRA gene, *GAD67*, are predominantly expressed by nonproliferative cells, although we cannot completely exclude the possibility that expression of these genes is associated with immature cells that turn over slowly and, thus, would be poorly labeled by BrdU. The results prompt us to propose a fascinating hypothesis that promiscuous gene expression is achieved by induction of heterogeneity among terminally differentiated mTECs rather than by multipotentiality of mTEC progenitors. We speculate that Aire may contribute to mTEC heterogeneity by acting on mTECs at the late differentiation stages and that lack of Aire may result in failure to create this heterogeneity. According to this scenario, additional mechanisms for the development of Aire-dependent autoimmunity might be possible beyond reduced TRA expression from Aire-deficient mTECs, for instance, altered Ag processing and/or presentation capacity by Aire-deficient mTECs (12) and/or altered T cell development affecting establishment of the complete T cell repertoire. Study of the mechanisms underlying the Aire-dependent production of heterogeneity among mature mTECs might be a rewarding approach to elucidating the nature of the negative selection niche in the thymus.

MATERIALS AND METHODS

Mice. Aire/GFP knock-in mice (RIKEN Center for Developmental Biology accession No. CDB0483K) were generated by gene targeting as described previously (32). In brief, the targeting vector was constructed by replacing the genomic *Aire* locus starting from exon 1 (immediately after the Kozak sequence) to exon 2 with a GFP-neomycin resistance (neo^r) gene cassette (20). The neo^r gene cassette harbors loxP sites at both ends. The targeting vector was introduced into TT2 embryonic stem cells (33), and the homologous recombinant clones were first identified by PCR and confirmed by Southern blot analysis. After the targeted cells had been injected into morula-stage embryos, the resulting chimeric male mice were mated with C57BL/6 females (CLEA) to establish germ-line transmission. *Aire*$^{+/GFP-neo}$ mice were crossed with Ayu1-Cre mice (21), a general deleter Cre recombinase-expressing transgenic line, to remove the neo^r gene cassette. After confirming removal of the neo^r gene cassette, mice were crossed with C57BL/6 mice to select the line containing the GFP knock-in allele but not the Cre recombinase-expressing transgene. *Aire*$^{+/GFP}$ mice were then crossed to obtain *Aire*$^{GFP/GFP}$ mice, which have the null mutation for the *Aire* gene. GAD67/GFP knock-in mice were heterozygous for GAD67-GFP (Δneo) as described previously (34). OT-II transgenic mice (35) were purchased from The Jackson Laboratory. The mice were maintained under pathogen-free conditions.

Published November 17, 2008

The protocols used in this study were in accordance with the Guidelines for Animal Experimentation of Tokushima University School of Medicine and were conducted with the approval of the RIKEN Kobe Animal Experiment Committee.

Immunohistochemistry. Mice were killed and the thymus tissues were fixed as described previously (25, 36). Immunohistochemical analysis of the thymus with UEA-1 (Vector Laboratories), rat anti-EpCAM mAb (BD), and rabbit polyclonal anti-K5 Ab (Covance) was performed as described previously (37). Rabbit polyclonal anti-Aire Ab was produced as described previously (13). Goat polyclonal anti-GFP Ab (Novus Biologicals) and rabbit polyclonal anti-GFP Ab (Invitrogen) were used for the detection of GFP-expressing cells. BrdU incorporation by mTECs was examined 4 h after i.p. injection of 1 mg BrdU/mouse, and the detection of BrdU incorporation was performed with anti-BrdU Ab (BD), as described previously (26). Rabbit polyclonal anti-p63 Ab was purchased from Santa Cruz Biotechnology, Inc. The level of cell shape complexity for each GFP^+ cell was calculated by dividing the length of the cellular periphery by the cell area (i.e., periphery/area $\times$ $1/4\pi$) measured by the WinROOF program (Mitani Corporation). After obtaining photos of the thymus sections stained with anti-GFP Ab, the photos were subjected to analysis with the software. Immunohistochemistry of the thymus sections and statistical analysis of cell shape complexity from different genotype of mice for comparison were processed simultaneously in the same set of experiment to minimize variability between the assays. Numbers of involucrin-expressing mTECs were assessed after staining the thymus sections with rabbit polyclonal Ab against mouse involucrin (Covance). Well developed $EpCAM^+$ thymic medullas were examined for the presence of involucrin-expressing cells from several thymus sections obtained from individual mice.

TEC preparation and flow cytometric analysis. TECs were prepared as described previously (12). In brief, thymic lobes were isolated from mice and cut into small pieces. The fragments were gently rotated in RPMI 1640 medium (Invitrogen) supplemented with 10% heat-inactivated FCS (Invitrogen), 20 mM Hepes, 100 U/ml penicillin, 100 μg/ml streptomycin, and 50 μM 2-ME at 4°C for 30 min and dispersed further with pipetting to remove the majority of thymocytes. The resulting thymic fragments were digested with 0.125% collagenase D (Roche) and 10 U/ml DNase I (Roche) in RPMI 1640 at 37°C for 15 min. The supernatants, containing dissociated TECs, were saved, and the remaining thymic fragments were further digested with collagenase D and DNase I. This step was repeated twice, and the remaining thymic fragments were digested with 0.125% collagenase/dispase (Roche) and DNase I at 37°C for 30 min. The supernatants from this digest were combined with the supernatants from the collagenase digests, and the mixture was centrifuged for 5 min at 450 *g*. The cells were suspended in PBS, containing 5 mM EDTA and 0.5% FCS, and kept on ice until the staining. The cells were stained with anti-CD45 mAb (BD) and UEA-1 and subjected to flow cytometric cell sorting with a FACS Vantage (BD). Flow cytometric analysis was performed after staining the cells with anti-CD45 mAb, UEA-1, anti-$I\text{-}A^b$ (eBioscience), and anti-CD80 (eBioscience) mAbs with a FACSCalibur (BD) as described previously (13, 37).

Real-time PCR. RNA was extracted from sorted mTECs with RNeasy Mini kits (QIAGEN) and made into cDNA with cDNA Cycle kits (Invitrogen) according to the manufacturer's instructions. Real-time PCR for quantification of the *insulin 2*, *SAP1*, *CRP*, and *Hprt* genes was performed as described previously (12, 13). The primers and the probes are as follows: *insulin 2* primers, 5′-AGACCATCAGCAAGCAGGTC-3′ and 5′-CTGGTGCAGCACTGATCCAC-3′; *insulin 2* probe, 5′-FAM-CCCGGCAGAAGCGTGGCATT-3′; *SAP1* primers, 5′-ACTCCTTGTGTTGCTTGGTGTTT-3′ and 5′-TCGACTGAATCAGAGGAATCAACT-3′; *SAP1* probe, 5′-FAM-TTCACCAGCAGAATCAGCAGTTCCAGAA-3′; *CRP* primers, 5′-TACTCTGGTGCCTTCTGATCATGA-3′ and 5′-GGCTTCTTTGACTCTGCTTCCA-3′; *CRP* probe, 5′-FAM-CAGCTTCTCTCGGACTTTTGGTCATGA-3′; *Hprt* primers, 5′-TGAAGAGCTACTGTAATGATCAGTCAAC-3′ and 5′-AGCAAGCTTGCAACCTTAACCA-3′; and *Hprt* probe, 5′-FAM-TGCTTTCCCTGGTTAAGCAGTACAGCCC-3′.

Statistical analysis. All results are expressed as mean ± SEM. Statistical analysis was performed using Student's two-tailed unpaired *t* test for comparisons between two groups. Differences were considered significant if p-values were 0.05 or less.

Online supplemental materials. Fig. S1 shows Aire-expressing cells in adult and embryonic thymi. Fig. S2 shows altered morphology together with the distribution of GFP^+ Aire-less mTECs in $Aire^{GFP}$ mice. Fig. S3 shows altered morphology together with the distribution of GFP^+ Aire-less mTECs in $Aire^{-/-}$ mice expressing the nonautoreactive OT-II TCR transgene. Fig. S4 shows altered morphology of GFP^+ Aire-less mTECs in $Aire^{GFP/GFP}$ mice at neonatal stage P1. Table S1 shows detailed information for mice analyzed for involucrin-expressing mTECs. Online supplemental material is available at http://www.jem.org/cgi/content/full/jem.20080046/DC1.

We thank Drs. Y. Hamazaki, E.A. Robey and A.G. Farr for suggestions on immunohistochemistry.

This work was supported in part by Grants-in-Aid for Scientific Research from the Japan Society for the Promotion of Science and from the Ministry of Education, Culture, Sports, Science and Technology of Japan, and by Health and Labor Sciences Research Grants, Research on Psychiatric and Neurological Diseases and Mental Health (M. Matsumoto).

The authors have no conflicting financial interests.

Submitted: 7 January 2008
Accepted: 17 October 2008

REFERENCES

1. Kamradt, T., and N.A. Mitchison. 2001. Tolerance and autoimmunity. *N. Engl. J. Med.* 344:655–664.
2. Björses, P., J. Aaltonen, N. Horelli-Kuitunen, M.L. Yaspo, and L. Peltonen. 1998. Gene defect behind APECED: a new clue to autoimmunity. *Hum. Mol. Genet.* 7:1547–1553.
3. Pitkänen, J., and P. Peterson. 2003. Autoimmune regulator: from loss of function to autoimmunity. *Genes Immun.* 4:12–21.
4. Björses, P., M. Pelto-Huikko, J. Kaukonen, J. Aaltonen, L. Peltonen, and I. Ulmanen. 1999. Localization of the APECED protein in distinct nuclear structures. *Hum. Mol. Genet.* 8:259–266.
5. Heino, M., P. Peterson, J. Kudoh, K. Nagamine, A. Lagerstedt, V. Ovod, A. Ranki, I. Rantala, M. Nieminen, J. Tuukkanen, et al. 1999. Autoimmune regulator is expressed in the cells regulating immune tolerance in thymus medulla. *Biochem. Biophys. Res. Commun.* 257:821–825.
6. Hogquist, K.A., T.A. Baldwin, and S.C. Jameson. 2005. Central tolerance: learning self-control in the thymus. *Nat. Rev. Immunol.* 5:772–782.
7. Kyewski, B., and L. Klein. 2006. A central role for central tolerance. *Annu. Rev. Immunol.* 24:571–606.
8. Derbinski, J., A. Schulte, B. Kyewski, and L. Klein. 2001. Promiscuous gene expression in medullary thymic epithelial cells mirrors the peripheral self. *Nat. Immunol.* 2:1032–1039.
9. Anderson, M.S., E.S. Venanzi, L. Klein, Z. Chen, S.P. Berzins, S.J. Turley, H. von Boehmer, R. Bronson, A. Dierich, C. Benoist, and D. Mathis. 2002. Projection of an immunological self shadow within the thymus by the aire protein. *Science.* 298:1395–1401.
10. Derbinski, J., J. Gabler, B. Brors, S. Tierling, S. Jonnakuty, M. Hergenhahn, L. Peltonen, J. Walter, and B. Kyewski. 2005. Promiscuous gene expression in thymic epithelial cells is regulated at multiple levels. *J. Exp. Med.* 202:33–45.
11. Liston, A., D.H. Gray, S. Lesage, A.L. Fletcher, J. Wilson, K.E. Webster, H.S. Scott, R.L. Boyd, L. Peltonen, and C.C. Goodnow. 2004. Gene dosage–limiting role of *Aire* in thymic expression, clonal deletion, and organ-specific autoimmunity. *J. Exp. Med.* 200:1015–1026.
12. Kuroda, N., T. Mitani, N. Takeda, N. Ishimaru, R. Arakaki, Y. Hayashi, Y. Bando, K. Izumi, T. Takahashi, T. Nomura, et al. 2005. Development

of autoimmunity against transcriptionally unrepressed target antigen in the thymus of Aire-deficient mice. *J. Immunol.* 174:1862–1870.

13. Niki, S., K. Oshikawa, Y. Mouri, F. Hirota, A. Matsushima, M. Yano, H. Han, Y. Bando, K. Izumi, M. Matsumoto, et al. 2006. Alteration of intra-pancreatic target-organ specificity by abrogation of Aire in NOD mice. *J. Clin. Invest.* 116:1292–1301.
14. Anderson, M.S., E.S. Venanzi, Z. Chen, S.P. Berzins, C. Benoist, and D. Mathis. 2005. The cellular mechanism of Aire control of T cell tolerance. *Immunity.* 23:227–239.
15. Devoss, J., Y. Hou, K. Johannes, W. Lu, G.I. Liou, J. Rinn, H. Chang, R. Caspi, L. Fong, and M.S. Anderson. 2006. Spontaneous autoimmunity prevented by thymic expression of a single self-antigen. *J. Exp. Med.* 203:2727–2735.
16. Matsumoto, M. 2007. Transcriptional regulation in thymic epithelial cells for the establishment of self tolerance. *Arch. Immunol. Ther. Exp. (Warsz.).* 55:27–34.
17. Gillard, G.O., and A.G. Farr. 2006. Features of medullary thymic epithelium implicate postnatal development in maintaining epithelial heterogeneity and tissue-restricted antigen expression. *J. Immunol.* 176:5815–5824.
18. Gillard, G.O., J. Dooley, M. Erickson, L. Peltonen, and A.G. Farr. 2007. Aire-dependent alterations in medullary thymic epithelium indicate a role for Aire in thymic epithelial differentiation. *J. Immunol.* 178:3007–3015.
19. Gillard, G.O., and A.G. Farr. 2005. Contrasting models of promiscuous gene expression by thymic epithelium. *J. Exp. Med.* 202:15–19.
20. Moriguchi, T., M. Hamada, N. Morito, T. Terunuma, K. Hasegawa, C. Zhang, T. Yokomizo, R. Esaki, E. Kuroda, K. Yoh, et al. 2006. MafB is essential for renal development and F4/80 expression in macrophages. *Mol. Cell. Biol.* 26:5715–5727.
21. Niwa, H., K. Araki, S. Kimura, S. Taniguchi, S. Wakasugi, and K. Yamamura. 1993. An efficient gene-trap method using poly A trap vectors and characterization of gene-trap events. *J. Biochem.* 113:343–349.
22. Fuchs, E. 1990. Epidermal differentiation. *Curr. Opin. Cell Biol.* 2:1028–1035.
23. Hale, L.P., and M.L. Markert. 2004. Corticosteroids regulate epithelial cell differentiation and Hassall body formation in the human thymus. *J. Immunol.* 172:617–624.
24. Patel, D.D., L.P. Whichard, G. Radcliff, S.M. Denning, and B.F. Haynes. 1995. Characterization of human thymic epithelial cell surface antigens: phenotypic similarity of thymic epithelial cells to epidermal keratinocytes. *J. Clin. Immunol.* 15:80–92.
25. Maemura, K., Y. Yanagawa, K. Obata, T. Dohi, Y. Egashira, Y. Shibayama, and M. Watanabe. 2006. Antigen-presenting cells expressing glutamate decarboxylase 67 were identified as epithelial cells in glutamate decarboxylase 67-GFP knock-in mouse thymus. *Tissue Antigens.* 67:198–206.
26. Hamazaki, Y., H. Fujita, T. Kobayashi, Y. Choi, H.S. Scott, M. Matsumoto, and N. Minato. 2007. Medullary thymic epithelial cells expressing Aire represent a unique lineage derived from cells expressing claudin. *Nat. Immunol.* 8:304–311.
27. Gray, D., J. Abramson, C. Benoist, and D. Mathis. 2007. Proliferative arrest and rapid turnover of thymic epithelial cells expressing Aire. *J. Exp. Med.* 204:2521–2528.
28. Senoo, M., F. Pinto, C.P. Crum, and F. McKeon. 2007. p63 Is essential for the proliferative potential of stem cells in stratified epithelia. *Cell.* 129:523–536.
29. Akiyoshi, H., S. Hatakeyama, J. Pitkänen, Y. Mouri, V. Doucas, J. Kudoh, K. Tsurugaya, D. Uchida, A. Matsushima, K. Oshikawa, et al. 2004. Subcellular expression of autoimmune regulator (AIRE) is organized in a spatiotemporal manner. *J. Biol. Chem.* 279:33984–33991.
30. Rossi, S.W., M.Y. Kim, A. Leibbrandt, S.M. Parnell, W.E. Jenkinson, S.H. Glanville, F.M. McConnell, H.S. Scott, J.M. Penninger, E.J. Jenkinson, et al. 2007. RANK signals from CD4^{+}3^{-} inducer cells regulate development of Aire-expressing epithelial cells in the thymic medulla. *J. Exp. Med.* 204:1267–1272.
31. Liu, Y.J. 2006. A unified theory of central tolerance in the thymus. *Trends Immunol.* 27:215–221.
32. Murata, T., K. Furushima, M. Hirano, H. Kiyonari, M. Nakamura, Y. Suda, and S. Aizawa. 2004. *ang* is a novel gene expressed in early neuroectoderm, but its null mutant exhibits no obvious phenotype. *Gene Expr. Patterns.* 5:171–178.
33. Yagi, T., T. Tokunaga, Y. Furuta, S. Nada, M. Yoshida, T. Tsukada, Y. Saga, N. Takeda, Y. Ikawa, and S. Aizawa. 1993. A novel ES cell line, TT2, with high germline-differentiating potency. *Anal. Biochem.* 214:70–76.
34. Tamamaki, N., Y. Yanagawa, R. Tomioka, J. Miyazaki, K. Obata, and T. Kaneko. 2003. Green fluorescent protein expression and colocalization with calretinin, parvalbumin, and somatostatin in the GAD67-GFP knock-in mouse. *J. Comp. Neurol.* 467:60–79.
35. Barnden, M.J., J. Allison, W.R. Heath, and F.R. Carbone. 1998. Defective TCR expression in transgenic mice constructed using cDNA-based alpha- and beta-chain genes under the control of heterologous regulatory elements. *Immunol. Cell Biol.* 76:34–40.
36. Kusser, K.L., and T.D. Randall. 2003. Simultaneous detection of EGFP and cell surface markers by fluorescence microscopy in lymphoid tissues. *J. Histochem. Cytochem.* 51:5–14.
37. Kajiura, F., S. Sun, T. Nomura, K. Izumi, T. Ueno, Y. Bando, N. Kuroda, H. Han, Y. Li, A. Matsushima, et al. 2004. NF-κB-inducing kinase establishes self-tolerance in a thymic stroma-dependent manner. *J. Immunol.* 172:2067–2075.

Disease Markers 25 (2008) 27–35
IOS Press

Molecular network analysis of T-cell transcriptome suggests aberrant regulation of gene expression by NF-κB as a biomarker for relapse of multiple sclerosis

Jun-ichi Satoh[a,b,*], Tamako Misawa[a], Hiroko Tabunoki[a] and Takashi Yamamura[b]
[a]*Department of Bioinformatics and Molecular Neuropathology, Meiji Pharmaceutical University, Japan*
[b]*Department of Immunology, National Institute of Neuroscience, NCNP, Japan*

Abstract. Molecular mechanisms responsible for acute relapse of multiple sclerosis (MS) remain currently unknown. The aim of this study is to identify the relapse-specific biomarker genes in T lymphocytes of relapsing-remitting MS (RRMS). Total RNA of $CD3^+$ T cells isolated from six RRMS patients taken at the peak of acute relapse and at the point of complete remission was processed for DNA microarray analysis. We identified a set of 43 differentially expressed genes (DEG) between acute relapse and complete remission. By using 43 DEG as a discriminator, hierarchical clustering separated the cluster of relapse from that of remission. The molecular network of 43 DEG investigated by KeyMolnet, a bioinformatics tool for analyzing molecular interaction on the curated knowledge database, showed the most significant relationship with aberrant regulation of gene expression by the nuclear factor-kappa B (NF-κB) in T cells during MS relapse. These results support the logical hypothesis that NF-κB plays a central role in triggering molecular events in T cells responsible for induction of acute relapse of MS, and suggest that aberrant gene regulation by NF-κB on T-cell transcriptome might serve as a molecular biomarker for monitoring the clinical disease activity of MS.

Keywords: KeyMolnet, multiple sclerosis, nuclear factor-kappa B, relapse, T cells

1. Introduction

Multiple sclerosis (MS) is an inflammatory demyelinating disease of the central nervous system (CNS) white matter mediated by an autoimmune process triggered by a complex interplay of both genetic and environmental factors [1]. The great majority of MS patients show a relapsing-remitting (RR) clinical course. Intravenous administration of interferon-gamma (IFNγ) to MS patients provoked acute relapses accompanied by activation of the systemic immune response, indicating a pivotal role of proinflammatory T helper type 1 (Th1) lymphocytes in the immunopathogenesis of RRMS [2]. More recent studies proposed the pathogenic role of Th17 lymphocytes in sustained tissue damage in MS [3]. Several studies showed an etiological implication of viral infections for induction of acute relapse of MS [4]. However, the involvement of any viruses in MS relapse is not fully validated. A recent study showed that a methylprednisolone pulse therapy immediately reduces the levels of activated p65 subunit of the nuclear factor-kappa B (NF-κB) in lymphocytes of MS patients, suggesting a key role of NF-κB in induction of acute relapse of MS [5]. Furthermore, IFNγ is identified as one of NF-κB target genes, while IFNβ treatment attenuates proinflammatory responses in T cells by inhibiting the NF-κB activity [6,

*Corresponding author: Prof. Dr. Jun-ichi Satoh, Department of Bioinformatics and Molecular Neuropathology, Meiji Pharmaceutical University, 2-522-1 Noshio, Kiyose, Tokyo 204-8588, Japan. Tel./Fax: +81 42 495 8678; E-mail: satoj@my-pharm.ac.jp.

ISSN 0278-0240/08/$17.00

7]. At present, the precise molecular mechanism underlying MS relapse remains almost unknown. If the molecular biomarkers for MS relapse are identified, we could predict the timing of relapses, being highly valuable to start the earliest preventive intervention.

DNA microarray technology is a novel approach that allows us to systematically monitor the expression of a large number of genes in disease-affected tissues and cells. It has given new insights into molecular mechanisms promoting the autoimmune process in MS, and has made it possible to identify biomarkers for monitoring the clinical outcome [8]. The comprehensive gene expression profiling of MS brain tissues and peripheral blood lymphocytes identified a battery of genes deregulated in MS, whose role has not been previously predicted in its pathogenesis [9–12]. By microarray analysis, we recently identified a set of interferon-responsive genes expressed in highly purified peripheral blood $CD3^+$ T cells of RRMS patients receiving treatment with interferon-beta (IFNβ) [13]. IFNβ immediately induces a burst of expression of chemokine genes with potential relevance to IFNβ-related early adverse effects in MS [14]. The majority of differentially expressed genes in $CD3^+$ T cells between untreated MS patients and healthy subjects were categorized into apoptosis signaling regulators [15]. Furthermore, we found that T-cell gene expression profiling classifies a heterogeneous population of Japanese MS patients into four distinct subgroups that differ in the disease activity and therapeutic response to IFNβ [16].

In the present study, to identify MS relapse-specific biomarker genes, we conducted DNA microarray analysis of peripheral blood $CD3^+$ T cells isolated from RRMS patients taken at the peak of acute relapse and at the point of complete remission of the identical patients. We focused highly purified $CD3^+$ T cells because autoreactive pathogenic and regulatory cells, which potentially play a major role in MS relapse and remission, might be enriched in this fraction. Since microarray analysis usually produces a large amount of gene expression data at one time, it is often difficult to find out the meaningful relationship between gene expression profile and biological implications from such a large quantity of available data. To overcome this difficulty, we have made a breakthrough to identify the molecular network most closely associated with DNA microarray data by a novel data-mining tool of bioinformatics named KeyMolnet.

2. Subjects and methods

2.1. Blood samples

The present study included 6 Japanese women presenting with clinically active RRMS, diagnosed by certified neurologists of Department of Neurology, Musashi Hospital, National Institute of Neuroscience, National Center of Neurology and Psychiatry (NCNP), according to the established criteria [17]. Written informed consent was obtained from all the patients. The Ethics Committee of NCNP approved the present study. The patients showed the mean age of 41 ± 12 years and the mean Expanded Disability Status Scale (EDSS) score of 1.8 ± 0.5 (Fig. 1). None of the patients received treatment with glatiramer acetate, mitoxantrone or other immunosuppressants at any time in the entire clinical course. None of them were given methylprednisolone or interferons at least for three weeks before the time point of blood sampling. Blood samples of individual patients taken at two time points were compared, one at the point of complete remission and the other at the peak of acute relapse, usually on the day of onset or one day after acute relapse, just before starting treatment with intravenous methylprednisolone pulse (IVMP) or oral administration of high dose prednisolone (Fig. 1). The comprehensive clinical and neuroradiological evaluation on each case satisfied characteristics of either relapse or remission of MS.

2.2. Microarray analysis

The present study utilized a custom microarray containing duplicate spots of 1,258 cDNA, which were carefully designed by excluding any cross-hybridization, generated by PCR, and immobilized on a poly-L-lysine-coated slide glass (Hitachi Life Science, Kawagoe, Saitama, Japan) [13–16]. The array contains well-annotated biologically important human genes of various functional classes, which cover a wide range of cytokines/growth factors and their receptors, apoptosis regulators, oncogenes, transcription factors, signal transducers, cell cycle regulators and housekeeping genes (see the reference [14] for the complete gene list).

Peripheral blood mononuclear cells (PBMC) were isolated from 30 ml of heparinized blood by centrifugation on a Ficoll density gradient. They were labeled with anti-CD3 antibody-coated magnetic microbeads (Miltenyi Biotec, Auburn, CA), and $CD3^+$ T cells were separated by AutoMACS (Miltenyi Biotec). The puri-